figure 3-26

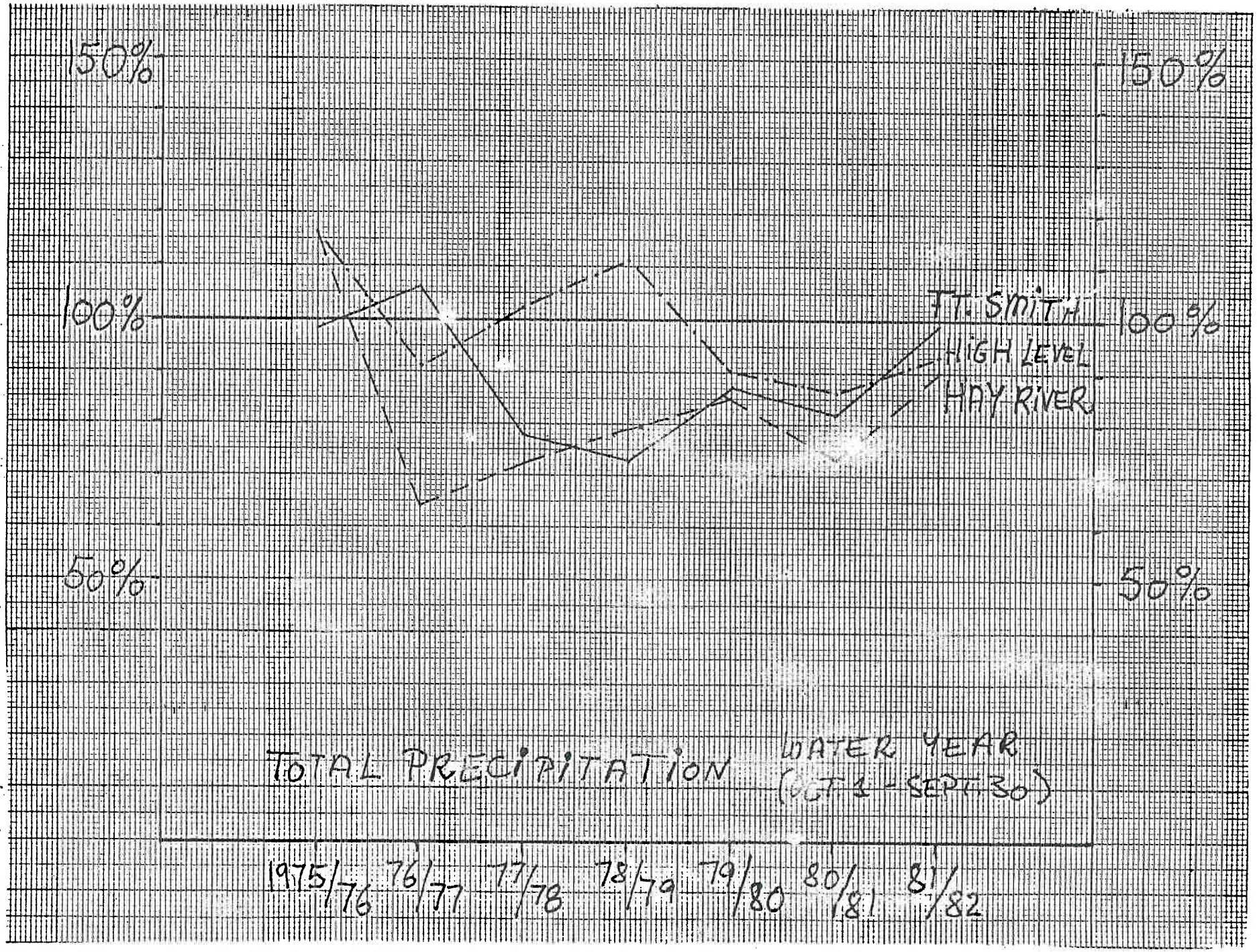
150%
100%
50%
FT. SMITH
HIGH LEVEL
HAY RIVER
TOTAL PRECIPITATION
WATER YEAR
(OCT 1 - SEPT 30)
1975/76
76/77
77/78
78/79
79/80
80/81
81/82

Fig. 3-20

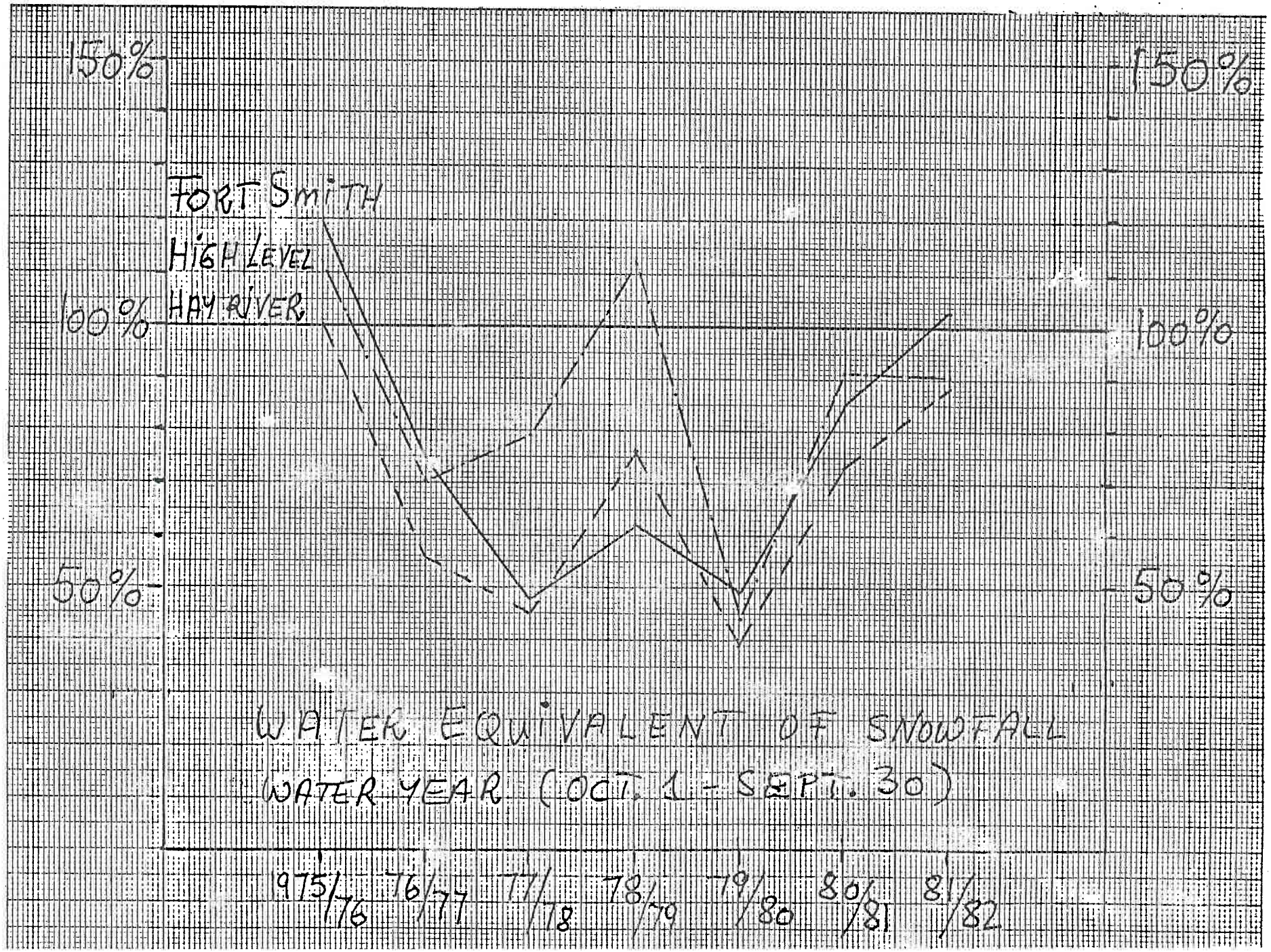
150%
100%
50%
FORT SMITH
HIGH LEVEL
HAY RIVER
WATER EQUIVALENT OF SNOWFALL
WATER YEAR (OCT. 1 - SEPT. 30)
1975/76
76/77
77/78
78/79
79/80
80/81
81/82

Fig. 3-2d

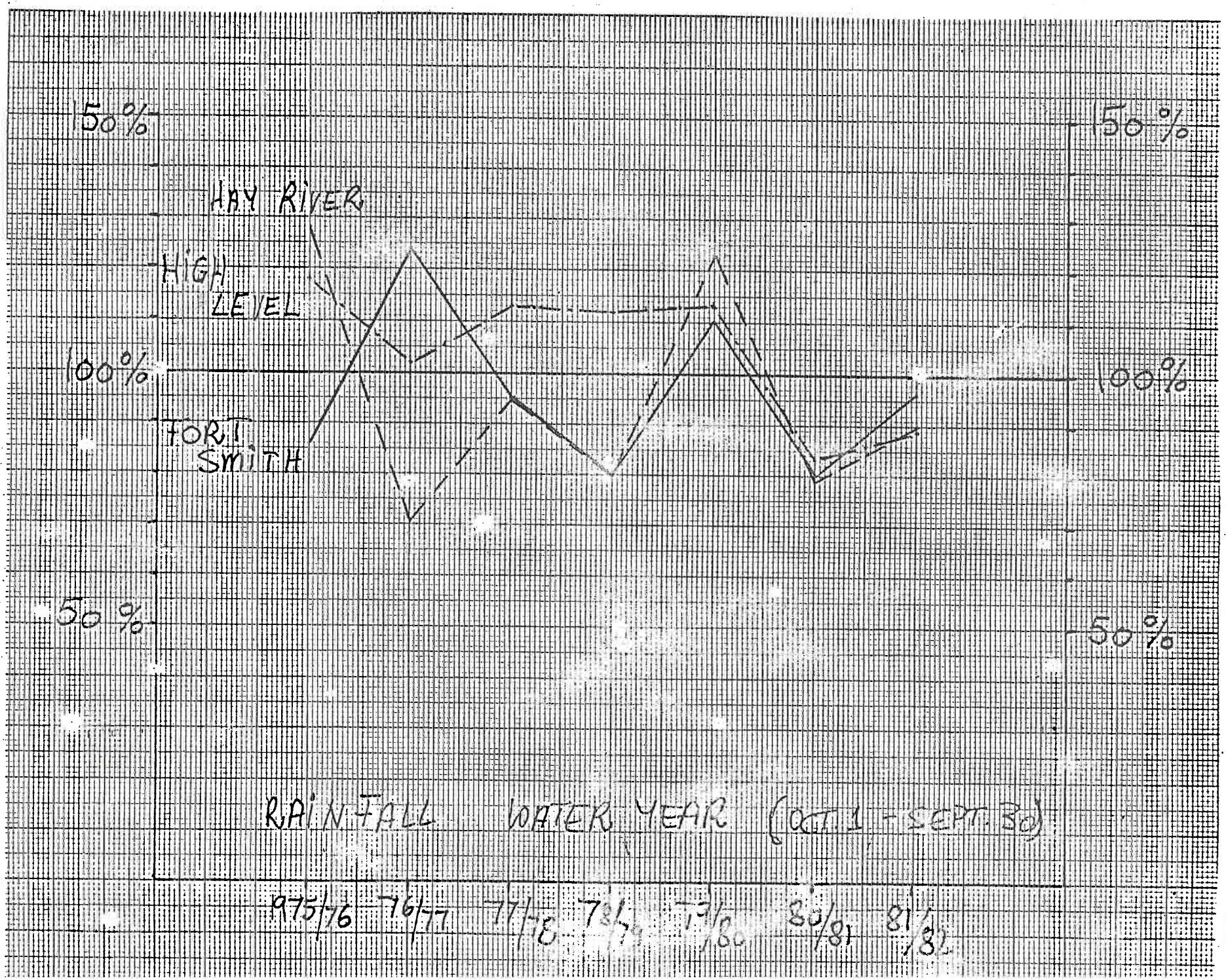
150%
HAY RIVER
HIGH LEVEL
100%
FORT SMITH
50%
150%
100%
50%
RAINFALL WATER YEAR (OCT. 1 - SEPT. 30)
75/76
76/77
77/78
78/79
79/80
80/81
81/82

the areal spread of the wider-spaced oil wells is recorded in figure 3-3.

FIGURE 3-2

FIGURE 3-3

Both figures are based on the compilation of borehole data listed in Appendix 2. Figure 3-2B shows the boreholes geologically evaluated by computer data processing. Time limitations prevented the inclusion of all available boreholes into the computer data banks. Data editing also had to be curtailed because of managerial directives.

SURFICIAL GEOLOGY

The Caribou Mountains consist primarily of clastic Cretaceous rocks (Fig. 3-4), whereas the lowlands towards the north and east in the study area are mainly underlain by Upper and Middle Devonian calcareous, gypsiferous and other evaporitic rocks, often covered by quaternary sediments (Alberta Research Council, 1970; Douglas, 1974; Douglas and Norris, 1974).

FIGURE 3-4

The supposedly largest gypsum karst area in North America occurs in the lowlands between the Caribou Mountains and Pine Point. All sedimentary bedrock strata dip gently to the west; they are underlain by crystalline Precambrian rocks.

OVERBURDEN

Much of the overburden in the Pine Point area has been deposited by the Laurentide Ice Sheet less than 8 to 10 thousand years ago. The material is composed of till with accumulations of sand and gravel in some areas. Precambrian erratics and Devonian carbonates can be found

ubiquitous within the overburden and often as layers at the bottom of the overburden. In the past the existance of a hardpan layer was thought to be widespread. It appears certain by now that the hardpan layer is a more local phenomenon. It was not reported in borehole logs. If present, it imposed some problem in overburden removal at pits. The hardpan layer is probably caused by chemical precipitation of carbonates from the groundwater in the timespan from the last ice coverage to now.

Overburden thickness varies in the area from zero to more than 200 ft (Glm) in sinkholes (Fig. 3-5). Some sinkholes in the area and at orebodies are filled with Pleistocene material to even greater depth.

FIGURE 3-5

BEDROCK STRATIGRAPHY

A schematic stratigraphic comparison between parts of the study area and surrounding areas has been given by Meijer-Drees and Davies (1976), here reproduced as Figure 3-6.

FIGURE 3-6

Figure 3-7 shows a south to north cross-section from the Caribou Mountains to Great Slave Lake and the Horn Plateau presented by Meijer-Drees and Davies (1976).

FIGURE 3-7

Krebs (1982, unpublished manuscript) compiled the Phanerozoic stratigraphy and significant events in the Pine Point area (Fig. 3-8). Figure 3-9 shows the geological nomenclature adopted by this report for the evaluation of borehole logs.

FIGURE 3-8

FIGURE 3-9

FIGURE 3-10

Stratigraphic relationships at the Pine Point reef barrier and the schematic position of the known orebodies are shown in Figure 3-10. Figure 3-10 is a schematic N-S cross-section showing the projected positions of the orebodies. In reality the orebodies shown are positioned in a west-easterly direction as follows: A-70, Z-53N, K-57, O-42, M-40, W-17, X-15 and N-204.

It appears that the orebodies, from west to east, are positioned in increasingly lower stratigraphic levels. All orebodies shown are close to the present surface of the Paleozoic rocks, indicating that the ore-forming process may be related not so much to stratigraphic position as to the present surface of the Paleozoic rocks i.e. approximately the topographic surface.

TECTONICS

In the Precambrian rocks extensive fault zones are known to exist, as for example the McDonald Fault and Prebble Fault running in a NE to SW direction for more than 500 km (Kyle, 1981). Both faults appear to be related to the pronounced tectonic morphology of the east arm of Great Slave Lake.

FIGURE 3-11

Figure 3-11, based on the evaluation of large scale geomagnetic maps published by Douglas (1970), suggests that major N-S fault zones lead from the Caribou Mountains plateau into the area of Pine Point. In the Devonian strata overlying the Precambrian, post-Devonian tectonics are not well understood, because of the absence of late Paleozoic and

younger strata over most of the region (Kyle, 1981). The development of the Pine Point hinge zones (N65E) is related to Middle Devonian faulting and fracturing (Skall, 1975).

The hinge zones form a distinct angle with the McDonald Fault system in the Precambrian basement. Gentle folds bending parallel to the hinge zones are also present (Kyle, 1981). Exploration drilling by Abadena Oil indicated 15 m (50 ft) vertical displacements along a NE-SW system (fault A in Fig. 3-13A).

According to Kyle (1981) post-Amco displacements were recognized by Skall (1969).

De Wit et al. (1973) feel that the most important uplifts in the region took place during the late Paleozoic and early Mesozoic, and during the late Cretaceous and Tertiary. These tectonic movements may have caused further displacement along older fault zones, and they are responsible for the present southerly dip of the Pine Point barrier complex (Kyle, 1981).

Kesler et al. (1972) measured the strike of major vertical joints in open pits close to the Pine Point townsite. They identified NE-SW and SE-NW striking sets of joints (Figure 3-12).

Figure 3-12

Figure 3-13

A structure contour map of the E-shale (Fig. 3-13) documents the existance of NE-SW and SE-NW trending structures on a regional scale to the NE of the Pine Point townsite (arrows in Fig.3-13B) and confirms the subsurface observations made by Abedena Oil (fault A in Fig. 3-13B).

To the SW of Pine Point the map of the Amco-structures (Fig. 3-14) documents the existence of NW-SE and SW-NE trending structures which includes the direction of the hinge lines (compare arrows in Fig. 3-14 with Fig. 3-4). It also shows structures occurring along the Prebble Fault system and, in the area of Buffalo River, along a N-S trending system. The latter system coincides with the basement structure derived from the evaluation of aeromagnetic maps (Fig. 3-11).

Figure 3-14

Figure 3-15

The map of the bedrock surface of the Devonian carbonates (Fig. 3-15) confirms the above observations. But it should be noted that there is an additional NNE-SSW trending structure west of the Buffalo River (Fig. 3-15B). A "topographical" N-S feature exists in the surface of the bedrock along the N-S stretch of the Buffalo River. This structure apparently documents recent movement which affected both the Precambrian crystalline basement and the overlying Devonian rocks. This displacement was probably caused by isostatic rebound in response to the repeated retreats of the Laurentide Ice Sheet.

The map of overburden thickness (Fig. 3-5) shows numerous karstic features which, not surprisingly, follow major tectonic trends within the underlying rocks (see arrows in Fig. 3-5) as well as the slightly anomalous NNE - SSW trend (insert of Fig. 3-5).

In summary tectonic displacement in the Devonian rocks in the Pine Point area occurred not only along the hinge line system but also along the McDonald Fault system, and along N-S and NNE-SSW striking systems. Movement along all systems seems to have been revived by the Laurentide Ice Sheet, initially through associated depression and subsequently through isostatic rebound. The revived tectonic structures should provide flow paths for groundwater flow in the Devonian rocks as well as in the Precambrian basement.

PRESQU'ILE DOLOMITE

Both Norris (1965) and Richmond (1965) gave the Presqu'ile formational status not justified according to Skall (1975).

Skall (1975, p.32) defined 'Presqu'ile' "as coarsely crystalline dolomite, regardless of environmental conditions or time period of original carbonate deposition. Presqu'ile dolomite, which occurs between the Watt Mountain Formation and Facies B, D, E and J respectively, is termed Presqu'ile Facies or Facies K in this (his) report. Apart from occurring in Facies K, coarsely crystalline dolomite is also occasionally found in the top part of Facies B but rarely in the Watt Mountain or Slave Point Formations".

Since then, Pine Point geologists have extended the usage of the term Presqu'ile to include all typical coarsely crystalline dolomites as an indicator for a diagenetic recrystallization process, independent of stratigraphic position.

Within the Pine Point area proper the occurrences of Presqu'ile dolomite are thought to be confined to an area between the south and north hinge lines (Kyle,1981, Fig. 4; Macqueen and Powell, 1983, Fig. 2). The northern limit of the Presqu'ile coincides with the sudden appearance of the Buffalo River shale (Skall, 1975). To the south, the limit has been determined according to conventional cutoff of 1 ft (0.3 m) thickness (D. Adams, personal communication, 1982). Figure 3-16 shows variations of the thickness of the Presqu'ile Formation from 0 to more than 200 ft (60 m) to the east and west of Buffalo River.

FIGURE 3-16

FIGURE 3-17

An evaluation of our geological data bank shows the Presqu'ile cutting across the stratigraphic layers from the Pine Point Group in the east

to the stratigraphically much higher Slave Point Limestone in the west (Fig. 3-17 To the south, presqu'ilization has been reported close to the northern border of Wood Buffalo National Park.

Remnants of the green waxy Watt Mountain shale have been displaced into fractures and vugs of the Presqu'ile along the major collapse zone of the Pine Point Barrier reef (see Fig. 3-18).

FIGURE 3-18

Fritz and Jackson (1972) noted that coarsely crystalline dolostone contains less than 100 ppm Na as compared to contents of up to 600 ppm in the finely crystalline dolostone.

SUBSURFACE DISSOLUTION OF EVAPORITES

SUBSURFACE DISSOLUTION OF SALT BEDS

Occurrence of salt in the study area

In the Upper Mackenzie River area, two layers of salt occur in the Lower Devonian below the Chinchaga Formation, the Cold Lake salt and the Lotsberg salt (compare Fig. 3-6). Figure 3-19 shows the distribution of the deeper Lotsberg salt inferred from its occurrence in oil wells.

FIGURE 3-19

Closer to Pine Point the present extent of its occurrence is not known because of the lack of deeply penetrating boreholes. The Cold Lake salt occurs directly below the Chinchaga Formation. Figure 3-20 shows its present distribution in the Upper Mackenzie River area and in northern Alberta. Again, the scarcity of deep boreholes in the Pine

---

FIGURE 3-20

Point area does not allow an accurate determination of its present-day eastern limit of occurrence. Deep boreholes near Pine Point (Cominco G-4, Cominco G-1, Pyramid 202A) and towards the south (Iskut Little Buffalo K-22) did not encounter Cold Lake salt. It does occur some distance to the west, and beneath the Caribou Mountains farther south of Pine Point.

Upper Devonian Prairie Evaporite salts are found in northern Alberta (Fig. 3-21) and they occur below parts of the Caribou Mountains.

FIGURE 3-21

Farther north they are replaced by anhydrites and dolomites of the Muskeg Formation (Fig. 3-21), and still farther north the carbonate facies of the Pine Point Group replaces the Muskeg Formation (Fig. 3-21, compare Fig. 3-10).

Dissolution of Salt in the Prairie Provinces

Ongoing dissolution of salt beds was already recognized by Tyrell (1892) who calculated a daily dissolution rate of thirty-seven tons for the saline discharge of one brook in Manitoba alone. Cameron (1949) estimated an annual discharge of 50,000 - 100,000 tons of salt by the known brine springs in Manitoba. Van Everdingen (1971) estimated a total daily discharge of 3,000 metric tons of NaCl (slightly more than 1 million tons a year) when considering springs and subaqueous discharge. The 1 million tons of salt would be equivalent to a volume of 514,000 m^3 of salt.

Dissolution of salt in Saskatchewan has been discussed by DeMille et al. (1964) and Holter (1969). Holter (1969) summarized the work of Bishop (1954), Christiansen (1967), Christopher (1961), Saskatchewan Department of Mineral Resources (1965), DeMille et al. (1964), Kent (1968), Kupsch (1956), Lane (1959), Maycock (1967), Price (1963), Sawatzky et al. (1960), Streeton (1967), Wilson et al. (1963)

and Walker (1957) in an attempt to determine the areas and geological times of the occurrence of subsurface dissolution of salt. According to Holter (1969, Fig. 25), dissolution of salt beds started in central parts of the Western Canada Sedimentary Basin during the Middle Devonian and continued in restricted areas during the late Devonian and during Mississippian and Jurassic time. By far the most intensive dissolution of salt beds occurred since the Jurassic (ibid). Dissolution was most pronounced along the north-eastern edge of the sedimentary basin and towards the south of Saskatoon and southwest of Regina (ibid). Along its northwestern edge, a band of about 100 km width experienced complete removal of salt and subsequent collapse of overlying strata.

In Alberta, dissolution of salt beds was also concentrated along the northeastern edge of the Western Canada Sedimentary Basin close to the discharge areas of present-day regional groundwater flow systems. Carrigy (1959, Fig. 6) estimated that about 700 ft (210 m) of salt have been removed from the Fort McMurray area. He concluded (ibid, p. 22) that for the Elk Point Group containing the Prairie Evaporites "the thickness of the formation in the McMurray area has been modified by solution of halite and this has caused some deformation of the overlying Beaverhill Lake strata.....Features which are probably solution breccias have been recorded in the formation in the Bear Westmount No. 2 well. The structure contour map on the upper surface of the Elk Point evaporites sensu lato (ibid, Fig. 5) illustrates collapse structures."

Saline springs and artesian boreholes discharging the dissolved salt have been discussed earlier by Ells (1926). Hamilton (1971) showed how progressively deeper salt beds have been removed (Elk Point salt, Cold Lake salt and Lotsberg salt, see Fig. 3-22).

FIGURE 3-22

Dissolution of Salt Beds in the Upper Mackenzie River Area

Dissolution of salt beds in the Upper Mackenzie River area received attention only relatively recently. The Cold Lake Formation there has a maximum thickness of 117 m, with a net salt thickness of 102 m (Meijer-Drees and Davies, 1976). "The lithology of the Cold Lake salt is identical to the Lotsberg salt. It consists of clear, very coarse crystalline halite, the only visible impurities are minor amounts of red shaly material, either interstratified or dispersed within the crystal aggregate" (ibid p. 59). In the past, the salt extended much farther to the east than today and its thickness may have been much greater (Meijer-Drees, personal communication, 1982).

"The overlying beds of the Chinchaga Formation are reddish brown and are in part brecciated, indicating that some salt solution took place at the top of the salt" (Meijer-Drees and Davies, 1976, p. 60) "The northeastern limit of the salt is approximately a straight line on the map and is caused by salt solution in the Mirage Point and Bear Rock Formations along the outcrop edge near the Canadian Shield" (ibid. p. 60). Figure 3-23 shows the distribution of salt dissolution and associated collapse and brecciation northwest of Great Slave Lake.

FIGURE 3-23

In the area northwest of Great Slave Lake dissolution of salt is continuing as evidenced by the artesian discharge of saltwater at the 1922 oil well, Windy Point No. 1 (Table 1.3 and Fig. 4-3). Farther to the north, in the Lac Belot area, Cook and Aitken (1971) described cretaceous sandstone infilling of fossil sinkholes in the Bear Rock Formation, indicating the existence of active solution processes as long ago as the Cretaceous. van Everdingen (1981, p. 22) concluded that the solution process is active in the area west of Great Bear Lake.

Dissolution of Salt Beds in the Pine Point Area

Figure 3-23 suggests dissolution of Cold Lake salt and the subsequent collapse and brecciation of overlying strata in the Pine Point area. Ongoing salt dissolution has already been indicated by chemical analyses presented by Camsell (1917), Brandon (1965) and Weyer et al. (1979). Weyer et al. (1979) described discharge zones of saline water along the Salt River, Little Buffalo River and the south shore of Great Slave Lake. Saline water was also identified in the pump discharge from open pits at Pine Point Mines.

Investigation of cores of the boreholes Pyramid 202A and Iskut Little Buffalo K-22 confirmed the existence of solution breccia as the equivalent of the Cold Lake salt below the Chinchaga Formation (Fig. 3-24 and Appendix 3). According to Morrow and Meijer-Drees' (1981) descriptive classification (see Table 3.1) the fabric indicates a particulate rubble float breccia. Similar breccia also occurs in the boreholes Cominco G1 (963-1033 ft) and G4 (993-1067 ft) in equivalent position. A stratigraphic cross-section from Great Slave Lake to Wood Buffalo National Park (Fig. 3-25) shows that in the Pine Point area the same kind of collapse and breccia zone (Cold Lake equivalent) exists

---

FIGURE 3-24

FIGURE 3-25

---

near the edge of the Canadian Shield as is found in the Prairie provinces and northwest of Great Slave Lake. It is furthermore possible that a breccia zone occurring in Pyramid 202A and Iskut Little Buffalo K-22 below the Cold Lake equivalent, may be the equivalent of the Lotsberg salt known to exist in the Hay River area. From analogy with Saskatchewan, Alberta and the area northwest of Great Slave Lake, one may conclude that the solution zone in the Pine Point area could stretch for 80-100 km or more westwards from the edge of the Canadian Shield. As the thickness of the dissolved salt may well have exceeded 100 m,

progressive dissolution of the salt would have caused widespread subsidence and collapse in the area. Meijer-Drees and Davies (1976) show displacement of post Cold Lake strata due to dissolution in an area east of the Caribou Mountains (Fig. 3-26).

FIGURE 3-26

In general, the process of salt dissolution is of great importance for the development of highly permeable rocks. The process of salt solutioning probably was greatly enhanced during the Pleistocene by groundwater flow originating from the Laurentide Ice Sheet (see "Glacial events" in this Chapter and "Sulphur and hydrogen isotopes" in Chapter 4).

SUBSURFACE DISSOLUTION OF CARBONATES AND SULPHATES

The process of karstification is dealt with in detail further below. Widespread non-karstic dissolution of carbonates is documented by stylolitization in the carbonates of the Pine Point Group. For the Upper Devonian Redwater Reef in Alberta, Mossop (1972) concluded from data on stylolite amplitudes and distribution, that stylolitization accounted for a reduction of carbonate thickness by about 150 ft. The stylolitization process was enhanced by sediment loading. Late Cretaceous events caused the dissolution of about 50 ft. of carbonates.

Exact data on stylolites are not available for the Pine Point area. Widespread dissolution of carbonates in connection with stylolitization has occurred, however, and may have been of similar magnitude as found by Mossop (1972). It is probable that stylolitization did not exert a strong effect on today's permeability distribution.

In the process of salt dissolution groundwaters become more saline and this increases the solubility for anhydrite, gypsum and carbonates. The solubility of $CaSO_4$ increases by about an order of magnitude (see Fig. 3-27), as the ionic strength of a NaCl solution increases

---

FIGURE 3-27

---

from 0 to 3 molal at temperatures below 90°C. A further rise in the ionic strength of the NaCl solution from 3.0 to 4.0 molal causes a drop in the solubility.

As the dissolution process is still active, we were able to document this process in the hydrochemical results of our regional water sampling program (Fig. 3-28, data reported in Weyer and Horwood, 1979a, 1980b). The scatter in the left-hand side of the sulphate diagram depends on the availability of SO_4^{2-}. On the right hand side the expected decrease of SO_4^{2-}

FIGURE 3-28

---

solubility with extremely high NaCl concentrations (compare Fig. 3-27) appears to be reflected in out field data. In contrast, the HCO_3^- diagram reflects in relative modest increase in solubility with increasing ionic strength of the NaCl solution up to about 0.03 molal (∿ 1000 mg/l), followed by an apparent slight decrease in solubility. This slight reduction of HCO_3^- solubility is probably not caused by pH changes since the waters are strongly buffered at a pH close to 7.

In summary, it appears that the dissolution of halite leads to a subsequent strong dissolution of gypsum and anhydrite.

GLACIAL EFFECTS

GLACIAL EROSION AND SEDIMENTS

Stratigraphic evidence suggests the occurrence of at least two glaciations covering the Great Slave Lake region (Craig, 1965, p. 28). Stalker (1976) found evidence of 13 major ice-sheet-type glaciations to have reached

the Canadian Prairies. Subsequently it appears that in Canada at least 20, possibly 30, major glacial oscillations occurred during the last 2 to 2.5 million years, probably about 40 to 50,000 years apart (A. MacS. Stalker, 1983, personal communication). Magnetostratigraphic methods place the oldest ice sheet built up in the Pliocene (Odin, 1982; van Eysinga, 1978). Alternatively some researchers suggest shifting the Pliocene-Pleistocene boundary further back. All glaciations reaching the Pine Point area are likely to have caused erosion of overlying unconsolidated sediments and Devonian bedrock.

Evidence for strong glacial erosion is widespread. The occurrence of igneous erratics and carbonate pebbles immediately above the eroded Paleozoic rocks (Fig. 3-29A) indicates that considerable glacial erosion by ice took place in the Pine Point area as far west as oil wells Heart Lake No. 1 and Reef Creek G-15. The occurrence of igneous erratics at an elevation of about 1500 m in the Mackenzie Mountains (Hughes, 1972) would indicate ice thicknesses of more than 2,000 m for the Pine Point area. Igneous erratics were also found in sinkholes and in the orebody A-55 (see Fig. 3-29B).

FIGURE 3-29

The amount of glacial erosion is difficult to determine. A gross volumetric determination from glacial sediments deposited is unreliable because of the strong erosional activity of rivers in the Mackenzie drainage system. If one assumes that Devonian strata have covered the Precambrian rocks further to the east than they do today and also that the bulk of the material removed was eroded by the glacial ice, then one can prepare a rough estimate based on the slight southwestern dip of the Devonian strata. Maiklem (1971) estimated the position of the original edge of the Elk Point Basin to be about 150 km to the NE of the present edge of the Canadian Shield. Walcott (1970, p. 721) determined a regional dip to the southwest of about $4.4\ m \cdot km^{-1}$ or about 0.44%. From the above

consideration, erosion of several hundred metres would appear possible. The occurrence of Hay River shale in a sinkhole more than 10 km from the nearest outcrop of Hay River shale would support an erosion of 100 m or more.

Sugden (1978, 1979) discussed the glacial erosion by the Laurentide Ice Sheet. The zone of maximum erosion forms an annulus between the centre of the former ice sheet and its periphery. The Pine Point area is positioned within this annulus in the "warm freezing" zone of Figure 3- 32.

The seemingly high amount of glacial erosion postulated here is in contrast to the previously held view of glacial geologists that the Laurentide Ice Sheet as well as the Fennoscandian Ice Sheet in Scandinavia only removed the regolith and smoothed the bedrock. Flint (1947, p. 81) stated: "It is doubtful whether the average thickness of rock removed from the Canadian Shield ...(is) more than a very few tens of feet". "Denial of deep erosion also stems from many instances where ice sheets passed over incoherent, weak stuffs without removing them (Prest, 1968)" according to White (1972). White (1972, p. 1037) points out, however, that " since some such occurrences are short distances up-glacier from obvious products of deep glacial erosion, such as the closed bedrock basins of the Great Lakes, it seems that ice sheets can be able or feckless erosive agents in the same place at different times." White (ibid.) in the same paper concludes that the Laurentide Ice Sheet caused considerable erosion.

Interpretation of Deep Sea Drilling Project results and air-gun seismic profiles from the North Atlantic (Laine, 1980) suggest an average glacial erosion of between 55 and 95 m of solid rock for North America and Southern Greenland.

Christiansen and Whitaker (1976) and Moran et al. (1980) stress the role of high-pressured groundwater discharge as cause of glacial thrusting through reduction of shearing resistance of the bed material.

These conditions would occur if basal water from beneath the ice sheet "was free to drain from the substrate through a conduit...[and] move[d] under a gradient of decreasing potential toward the margin of the glacier" (ibid., p. 471, 472). Sealing of the aquifer at the margin by a stratigraphic pinch-out or burial by glacial ice would cause the water pressure to be elevated high enough to cause shear failure in the substrate and blocks from the substrate would move along with the ice.

In the North American prairie "a complete gradation exists from blocks that were moved as little as 100 m and remained essentially intact to blocks that were moved many kilometers and, in many places, were thoroughly fragmented" (ibid., p. 472). Block sizes reported by Moran et al. (1980, Fig. 1) are up to 2.5 km^2 and 90 m high.

In the Pine Point area Hay River Shale overlies Devonian dolomite and may have caused a 'stratigraphic pinch-out situation'. Indeed erratic material has been identified within Hay River Shale (see Fig. 3-29B) either due to glacial thrusting or hydrodynamic blowout, discussed further below in this chapter.

Finally, just north of Pine Point is the Great Slave Lake, one of the bigger glacially eroded lakes on the Canadian Shield. In summary a glacial erosion in excess of 100 m appears likely in the Pine Point area.

Thicknesses of glacial till of up to 200 ft (61 m) are shown in the Pine Point area in Figure 3-5. Williams (1977) describes glacial deposits exceeding 800 ft (245 m) in thickness on the Horn Plateau about 100 km west of Great Slave Lake.

The role of groundwater in the process of glacial erosion has been further elucidated by Sugden and John (1976) and Sugden (1977, 1978, 1979). The occurrence of water at the bottom of glaciers facilitates the formation of warm-melting and warm-freezing zones below glaciers and ice caps. In Figure 3-30, erosion and entrainment are schematized by

---

FIGURE 3-30

---

a boulder train directed upwards into the glacier. The additional mass of ice is provided by freezing of groundwater originating in the warm-melting zone and elsewhere.

Sugden (1977) provided a physical reconstruction of the Laurentide Ice Sheet at its maximum, based on a mathematical model (Budd et al., 1970), encompassing a variety of climatological and physical data and boundary conditions. Although Budd's et al. (1970) model has been challenged recently on some finer mathematical points, the results of the model calculation would not change significantly if those points were incorporated into the model formulation (G. Holdsworth, oral communication, 1982). Figure 3-31 displays one of the results of Sugden's (1977) model calculation: the morphology of the ice sheet.

FIGURE 3-31

At Pine Point, the ice thickness was about 2,000 m at the maximum extension of the Laurentide Ice Sheet. The cretaceous plateaus of Caribou Mountains, Cameron Hills and Horn plateau were covered with ice.

FIGURE 3-32

With regard to basal erosion, Figure 3-32 indicates that the zone of warm-freezing would have covered the Pine Point area, where we suspected rather strong glacial erosion. It also covers part of the eroded portion of the Elk Point basin.

GROUNDWATER RECHARGE THROUGH GLACIERS AND ICE SHEETS

Basal melting of ice as discussed above, was a source for groundwater recharge into the underlying pre-Cambrian and Devonian strata. Sugden's (1977, Fig. 10) model-results indicated that between 0.5 and 1.0 mm a^{-1} basal ice melting could have occurred towards the east of Pine Point. Based on these numbers approximately 450-900 m^3 water could have been recharged per year into the underlying strata per square kilometer. This mechanism was the dominant cause for groundwater recharge below the interior part of the Laurentide Ice Sheet. However, within the peripheral warm-melting zone (Fig. 3-30, b, c; Fig. 3-32) of the Laurentide Ice Sheet, the basal melting was augmented by a substantial amount of water recharged through the ice from the surface of the ice sheet.

Glaciers and ice sheets have long been recognized as active groundwater systems by several authors. For temperate glaciers (ice temperature at the pressure melting point) measurements of basal water pressures have been reported by Mathews (1964), Vivian and Zumstein (1973), Hodge (1976, 1979), Kamb et al. (1979), Röthlisberger (1972, 1976), and Röthlisberger et al. (1979). Hodge's (1976) measurements showed a two-day lag time in the response of basal water pressures to large changes in water input at the glacier surface. Walder and Hallet (1979) describe deeply scalloped water channels and cavities in the bedrock surface below former glacier beds. Water spouts, discharging out of glaciers have been observed by many authors in alpine and arctic environments (Nordenskiöld, 1886; von Klebelsberg, 1948, p. 136-137, 375; Oechslin, 1955; Rucklidge, 1956, Wiseman, 1963 and Baranowski, 1973). Baranowski (1973, p. 132) concluded that geyser-like spouts of up to 60 m height, observed in 1957 on a glacier in Spitsbergen were caused by 12.2 mm of rainfall during the previous night and an associated snow ablation of 7 cm during the same 12 hour period. Recharging water had penetrated to the glacier bed. On its way to the snout of the glacier, water was dammed by cold

ice of the glacier front, a "subglacial lake or water pocket" (ibid.) formed, and the increasing pressure elevated and cracked the ice above the "lake", leading to a series of impressive geyser-like spouts.

For two alpine glaciers Collins (1979) determined subglacial and intraglacial groundwater flow in summer to be for both in the order of several cubic metres per second. Shreve (1972, p. 206) concluded that "water can move through a glacier in a manner somewhat analogous to the movement of groundwater through permeable cavernous limestone".

The example cited above refer mainly to temperate glaciers with ice temperature close to 0°C. They serve to clarify that, contrary to wide-spread opinion, glaciers often are a multiphase system with a very active groundwater component.

That these statements, to some degree, also hold true for so called cold-ice glaciers, with ice temperatures considerably below 0°C, has been shown by Müller and Iken (1973) and by Müller (1976) for the White Glacier on Axel-Heiberg Island. They report intraglacial and subglacial muddy and clear groundwater discharging at a rate of about 1.5 m^3/s along thrust planes on White Glacier in July 1968. Nearby ice temperatures were measured to be -5.5°C and -10°C respectively. Their findings illustrate the high degree of effectiveness of flowing water in glaciers and the existence of local warming of ice layers or cavities and fracture like systems in cold glaciers. Müller and Iken (1973) report also warm-melting conditions under part of the White Glacier.

Observations made by this author during the September 1982 Arctic Fjord cruise of the SS Hudson along the northeast coast of Baffin Island indicate that groundwater flow through cold glaciers does not seem to be an isolated occurrence. Significant amounts of groundwater were observed flowing in sediment-laden cavities, thrust planes and fractures at the broken-off face of Coronation Glacier in Coronation Fjord. This glacier outlets from Penny Ice Cap. Basal layers of temperate ice (30 m thickness) exist under the more northerly positioned Barnes Ice Cap (Classen, 1977).

It should be pointed out that even under the most severe climate conditions on earth, in Antarctica, basal melting of ice sheets has been inferred by the investigations of Budd et al. (1970), Budd (1971), Oswald and Robin (1973) and Dewart (1976). Literature on discharge of cold and warm groundwater into lakes and through a glacier in the Dry-Valley region of Antarctica has been reviewed by Weyer (1981

From the above it appears certain that considerable recharge [through and] from the Laurentide Ice Sheet should be taken into account when discussing paleo-groundwater flow in the Pine Point area.

The Laurentide Ice Sheet constituted a topographic high to the east of Pine Point, causing groundwater to flow from the east through Precambrian fault systems in the Devonian rocks towards Pine Point and beyond. Porosities and permeabilities were significantly enlarged for reasons outlined further below.

During interglacials, groundwater flow would have originated in the highlands to the south of Pine Point (Caribou Mountains and their foreland) passing through saline and anhydritic evaporites on its flow path towards the north. This flow configuration was probably similar to the present groundwater flow pattern described by Weyer et al. (1979) and in more detail in Chapter 4. In passing through the evaporites, groundwater is enriched in dissolved $CaSO_4$ and, in deeper layers, in dissolved NaCl as well.

During glacials, however, groundwater flow was from the east towards Pine Point and further to the west. The lack of gypsum and salt in the Devonian layers to the east of Pine Point would have caused a groundwater chemistry depleted in NaCl and $CaSO_4$.

CHEMISTRY OF GROUNDWATER IN FORMER 'SUBGLACIAL' ROCKS OF THE CANADIAN SHIELD.

Aqueous Ca-Na-Cl solutions have recently been found ubiquitous in Precambrian rocks on the Canadian Shield (Frape and Fritz, 1981 a, b, 1982, Fritz and Frape, 1982, Johnston, 1982). At Con Mine in Yellowknife, Frape and Fritz (1981b) described discharge rates of 1 to 3 l/s flowing for a long time from the Negus Fault and Pud Fault in 4500 ft (about 1370 m) depth. The waters have up to 214 g/l TDS at a temperature of about 23°C. $CaCl_2$ is the dominant species in the brines. Connection to the surface is suspected "because a progressive dilution with time by waters containing tritium, is noted" (ibid, p. 21). Similar mixings of 'old' Ca-Na-Cl brine and 'younger' water containing tritium occurs in about 900 m depth in mines of the Sudbury Basin (Frape and Fritz, 1982, p. 659). Generally, on the Canadian Shield brines occur at depth exceeding 600 to 1000 m (Frape and Fritz, 1981b, Fritz and Frape, 1982).

The origin of the brines is so far unknown. Frape and Fritz (1981b, 1982) list some possible sources:

1. Fossil sea water modified by
   - removal of Mg^{2+} during chloritization or the neoformation of other Mg-silicate
   - removal of K during the sericitization
   - relative increase of Ca^{2+} by ion-exchange between Ca^{2+} and Na^{-} during albitization of large quantities of Ca-plagioclase available in many parts of the shield ($2Na^{+} + CaAl_2Si_2O_8 + 4\ SiO_2 \rightarrow 2Na\ AlSi_3O_8 + Ca^{2+}$)
   - numerous other reactions not yet validated.

2. migration of sedimentary basin brines or formation waters
3. migration of waters from evaporite beds
4. brines as from ore deposition and metal bearing solutions
5. magmatic origin and
6. fluid inclusions.

None of the above mechanisms offer a satisfactory explanation according to Frape and Fritz (1981b, 1982). They concluded, however, that "there can be little doubt that the chemical characteristics and possibly the isotopic composition of these brines [are] controlled by extensive rock-water interactions "(Frape and Fritz, 1981 b). "The chemical evidence does not readily support any one specific origin or mode of evolution" (Frape and Fritz, 1982, p. 659).

However, "chemical analyses and specifically Br-concentration seem to suggest that the salt content of these brines is a primary feature. This would imply that saline waters have penetrated the Canadian Shield in the past.....It appears safe to assume that they cannot be generated in modern environments and are probably many millions of years old" (Frape and Fritz, 1981b, p. 29). "However, definite answers cannot be given since our studies so far have focussed only on the aqueous phase" (ibid., p. 28).

The suggested high age of the brines seems to exclude substantial glacial groundwater flow at depth through the Precambrian rocks on the Canadian Shield if no additional mechanism for the origin of the unique Ca-Na-Cl brines could be outlined. A tentative mechanism is, however, available and may be associated with groundwater flow beneath the Laurentide Ice Sheet and the erosional efficacy of ice sheets.

Firstly the possible origin of brines from fluid inclusion shall be examined. "Fluid inclusions constitute between 0.1 and 1 percent or even more (3% are reported by Roedder, 1972) of the rock volume, and from 0 to more than 50 percent by weight of the inclusion is salt (ibid, p. JJ3). "Fluid inclusions may also contribute as much as 100 ppm of each of several nonvolatile constituents to the total analysis of even 'pure' mineral separates" (ibid.,p. JJ3). Not enough fluid inclusion

studies on the Canadian Shield are available to allow a definite estimate of the average salinity of the fluid in the inclusions and the total volume of the fluid inclusions. Nevertheless, in light of a possible glacial erosion rate of more than 100 m, a substantial volume of saline waters and brine could have been released by the grinding action of the glacier and recharged into the deeper rock. Differential stress release movements associated with the ice sheet and the isostatic rebound would have opened additional fluid inclusions at fracture surfaces deep within the crystalline rocks. Assuming an average salt content of 20 percent and a volume of 1 percent of the rock for fluid inclusions, the released content of salt would be nearly equivalent to the dissolution of a salt layer of about 10 cm thickness spread over the Canadian Shield. From this estimate and the slow flow of groundwater at depth it appears that glacial erosion and differential movements on fractures may be viable mechanisms to generate a substantial part of the salt contents of the Ca-Na-Cl brines of the Canadian Shield by fluid release from fluid inclusions.

However, fluid released from the fluid inclusions would not necessarily contain sufficient amounts of Ca-ions. In the following we will discuss glacial processes which lead to supersaturation with respect to carbonate and silica in water at the glacier bed and also cause precipitation of carbonate and silica.

Several authors have shown that chemical processes are active under temperate glaciers by measuring dissolved ions in melt water and glacier ice as well as by investigating carbonate and silicate deposits precipitated by regelation from fluids at the bottom of glaciers at the lee surfaces of bedrock obstacles (Bauer, 1961; Keller and Reesman, 1963; Kers, 1964; Ford et al., 1970; Page, 1971; Reynolds and Johnson, 1972; Vivian and Zumstein, 1973; Hallet, 1975, 1976 a, b; Souchez and Lorrain, 1975, 1978; Hallet et al., 1978; Eyles et al., 1982). Although one might suspect chemical dissolution to be subdued in a glacial environment, Eyles et al. (1982) found the geochemical denudation rate in a glacier basin in northwest British Columbia to be substantially greater (947 mequiv m^{-2} a^{-1}) than the world average of 390 m E $m^{-2}a^{-1}$ (Livingstone, 1963). Calcium was accounting for nearly all of this loss (approx. 40 mg $m^{-2}a^{-1}$ Ca). Measured calcium concentrations in subglacial streams were up to 15 mg/l.

Dominant dissolution of Ca^{2+} and chemical denudation rates of 930 m equiv m^{-2} a^{-1} were also reported by Reynolds and Johnson (1972) for a glaciated Northern Cascade watershed. The study areas of Reynolds and Johnson (1972) and Eyles et al. (1982) were free of limestone and consisted of meta- and quartz diorites (Cascade Mountains), and of hornblende, granodiorite, volcanoclastics and derived epiclastics as well as some conglomerates and siltstones (Eyles et al., 1982). Reynolds and Johnson (1972) and Drever (1982) concluded for the Cascade watershed "that in the absence of both calcite in the bedrock and well defined clay mineral formation, the source may be slight but continuous and rapid alteration of primary minerals repeatedly exposed by glacier abrasion" (Eyles et al., 1982).

Having identified a possible source and mechanism for calcium generation at the bottom of the Laurentide Ice Sheet we will now search for a mechanism to concentrate weak Ca-solutionsto a brine. The investigations by Reynolds and Johnson (1972) and Eyles et al. (1982) were done in an area with high precipitation and hence enlarged groundwater flow through the glacier. Precipitation at the inland location of the Laurentide Ice Sheet must have been significantly lower thereby reducing water flow through the ice sheet. A comparatively lower amount of basal flow thus may have facilitated a significantly higher Ca-concentration than measured by Eyles et al. (1982).

Subglacial precipitation of calcite and silica by regelation at the bottom of glaciers is widespread (Bauer, 1961; Ford et. al. 1970; Page, 1971; Hallet, 1975; 1976 a, b). "Basal ice melts in zones of higher pressure and reduced temperature and the resulting water flows between the ice and bedrock towards zones of lower pressure and higher temperature, where it refreezes because of pressure reduction. As this water refreezes in areas of locally reduced pressure, generally along ice surfaces, solutes are continuously rejected into the liquid phase by the growing ice" (Hallet, 1975). The rest solution finally becomes supersaturated and mineral deposits are precipitated.

In the Alps, Bauer (1961) found $CaCO_3$ - aggregates of up to 40 * 40 * 1 cm extension precipiated on limestone by the receding ice within a time span considerably shorter than 300 years.

Souchez and Lorrain (1978) studied the Glacier de Tsijiore Nouve flowing on gneissic terrain of the Alps. They found that "hydrocarbonates and Ca-ions are present in the subglacial water, and therefore it is theoretically possible to reach by freezing the concentration level at which calcium carbonate will precipitate" (ibid., p. 324). From the chemical content of the basal ice layers they concluded however that precipitation of $CaCO_3$ did not occur. In the area of the Laurentide Ice Sheet calcium carbonate precipitation on gneissic rocks has been described by Hillaire - Marcel et al. (1979).

The freezing concentration mechanism described above might well be a viable source for higher concentrated Ca-solutions. A selective rejection of Ca in areas of silica precipitation might also occur. The mechanism may also be relevant in trying to explain the widespread occurrence of calcite and gypsum as fracture infilling in the granite of the Eye-Dashwa Lakes pluton near Atikokan, Ontario (Brown and McEwan, 1982; Kamineni and Dugal, 1982; Stone and Kamineni, 1982). Sources for sulphur would be available in the rocks. Carbon dioxide was available in the ice sheet which took it from the air and concentrated it by repeated refreezing of upper snow layers (Page, 1971).

In summation, it appears that the occurrence of highly saline Ca-Na-Cl solution on the Canadian Shield does not necessarily exclude significant and deeply penetrating groundwater flow from the Laurentide Ice Sheet

towards Pine Point. The conclusion of Frape and Fritz (1982) that saline waters of the Canadian Shield may be of Devonian sea-water origin and therefore have been at rest for millions of years may not be easily defendable. Frape and Fritz (1981 b, 1982) showed that fault zones at Yellowknife and in the Sudbury Basin do transmit modern water (age < 30 years) to depth exceeding 1000 m considerably.

ISOSTATIC REBOUND AND WATER LEVELS OF GLACIAL GREAT SLAVE LAKE (LAKE McCONNELL).

It has been shown that glaciation caused drastic changes in the direction of groundwater flow and the chemistry of groundwater. Post-glacial isostatic rebound and associated lake level changes of the ancestral Great Slave Lake caused saline solution to migrate upwards into non-saline layers which to date do not contain saline groundwaters. This was caused by an increase in the elevation of the discharge area. In Figure 3-33 the approximate southern boundary of the elevated discharge area is outlined by the coast line of glacial Great Slave Lake.

FIGURE 3-33

At this time all known orebodies in the Pine Point area must have been engulfed in gysiferous and saline water. In general, changes from saline to relatively fresh water and vice versa probably exerted a significant effect on rock porosity and permeability in the area, for reasons outlined further below.

Isostatic rebound in Canada has been described in theoretical studies by Andrews (1970) and Walcott (1970). In the Great Slave Lake area south of Pine Point, elevated beach lines indicate that the water level in Lake McConnell was approximately 400 ft (120 m) higher than it is at present. South of Pine Point, McGregor (1949, Fig. 1) and Craig (1965, p. 19) found beach lines at an elevation of about 925 feet (282 m) above sea level while the water level of Great Slave Lake now is approximately 513 ft (156 m) (see Fig. 3-34).

Pollohont /
livaly ebe.

POSITION				CAVITIES[1]					
				SULPHUR POINT LIMESTONE		PRESQU'ILE DOLOMITE Above C-1 Hrz.		PRESQU'ILE DOLOMITE Below C-1 Horz.	
Hole No.	Northing[2]	Easting[2]	Area	Size [cm]	Depth [feet]	Size [cm]	Depth [feet]	Size [cm]	Depth [feet]
118	61 957.1	55 980.7	E line	55	165.0				
169	77 849.4	54 372.8	X line			12.7	306.0		
239	72 139.7	63 418.7	W line					66.0	211.0
234	76 222.2	67 335.5	V line					38.1	254.0
352	78 305.9	85 908.2	D4W line					5.1	215.5
352	"	"	D4W line					14.0	222.5
329	80 087.9	85 048.7	D4W line	12.7	156.0				
329	"	"	D4W line	7.6	175.0				
308	80 633.0	85 980.9	D3W line					7.1	186.2
314	81 554.7	85 549.4	D3W line	8.4	140.2			15.2	174.0
314	"	"	D3W line	11.4	156.5				
77	79 948.1	90 050.6	D line					15.2	174.0
284	74 308.5	72 508.7	J1W line			7.6	84.4		
284	"	"	J1W line			8.9	135.5		
284	"	"	J1W line			7.6	168.5		
290	75 229.3	72 047.5	J1W line			10.2	165.0		
345	74 530.5	75 068.8	U4W line	10.2	127.5				
345	"	"	U4W line	5.1	134.0				
345	"	"	U4W line	>30.6	145.0				
307	76 568.8	75 055.4	U3W line					7.6	203.0
330	73 419.4	77 720.3	U2W line					24.1	215.5
213	79 089.5	77 462.7	U line					40.6	77.0
213	"	"	U line					11.4	120.5
272	79 613.1	90 872.6	D1E line					10.2	210.0
289	82 280.7	89 553.6	D1E line			83.8	106.0		
289	"	"	D1E line			10.2	151.0		
320	83 214.5	91 455.8	D3E line					5.1	157.0 (?)
176	87 668.1	109 186.1	Q line	22.9	112.0				
176	"	"	Q line	8.9	122.0				
176	"	"	Q line	30.2	127.0				
176	"	"	Q line	32.8	140.5				
176	"	"	Q line	>15.0	159.0				
455	92 668.7	117 022.2	P2W line					10.2	152.0
426	92 984.4	120 140.4	P1E line					10.2	114.0
426	"	"	P1E line					5.1	123.5
436	96 175.4	123 971.6	O1E line					7.6	64.0
466	96 599.7	124 829.8	O2E line					7.6	129.0
915	98 872.5	131 667.1	N4E line					15.2	52.0
876	102 006.9	131 301.8	N5E line					17.0	80.3 (?)
357	101 413.1	140 387.7	H line					10.2	81.5
361	81 595.9	88 150.9	K-60					25.4	201.0
366	85 025.4	104 241.7	N-50			10.2	159.0		
358	85 128.4	104 205.4	N-50					7.6	192.0
537	91 144.5	116 619.3	N-42					43.2	116.0
785	91 184.6	116 487.7	N-42					10.2	125.0
757	91 112.8	116 303.4	N-42			5.1	95.8		
757	"	"	N-42			5.1	100.0		
757	"	"	N-42			13.0	102.9		
539	91 343.4	116 094.9	N-42					7.6	102.0
508	91 170.2	116 174.8	N-42					8.6	128.6
779	91 265.2	115 910.4	N-42					25.4	122.0 (?)
821	90 953.5	115 940.0	N-42			6.3	59.5		
523	91 002.7	115 812.4	N-42					7.6	120.0
549	99 631.0	126 280.4	L-35					12.7	113.0
588	100 322.7	126 844.1	L-35					12.7	110.0
595	100 492.6	127 208.8	L-35					27.9	92.0
727	99 668.7	138 347.0	O-38					11.4	59.0
828	96 391.9	133 053.9	P-31					6.6	48.0
809	96 260.5	133 006.4	P-31			7.6	17.2	10.2	72.0
801	96 446.4	132 919.0	P-31			6.6	28.4		
801	"	"	P-31			6.6	35.0		
774	96 216.9	132 914.9	P-31			16.5	17.0		
789	96 403.5	132 833.0	P-31			25.4	67.9		
792	96 493.4	132 788.3	P-31			12.7	17.0		
751	96 179.2	132 822.1	P-31					7.6	64.4
751	"	"	P-31					7.6	97.0
735	96 361.7	132 739.3	P-31			10.2	31.0		
795	97 161.6	131 746.3	O-32					7.6	55.0
800	97 108.4	131 629.9	O-32			5.1	19.6		
800	"	"	O-32			7.6	51.0		
800	"	"	O-32			5.1	56.0		

1) Numerous other voids occurred, but most were less than 5 cm in width.
2) Pine Point Engineering coordinates
3) The C-1 horizon consists of a tongue of J-facies extending from the south into the main-trend.

FRACTURES

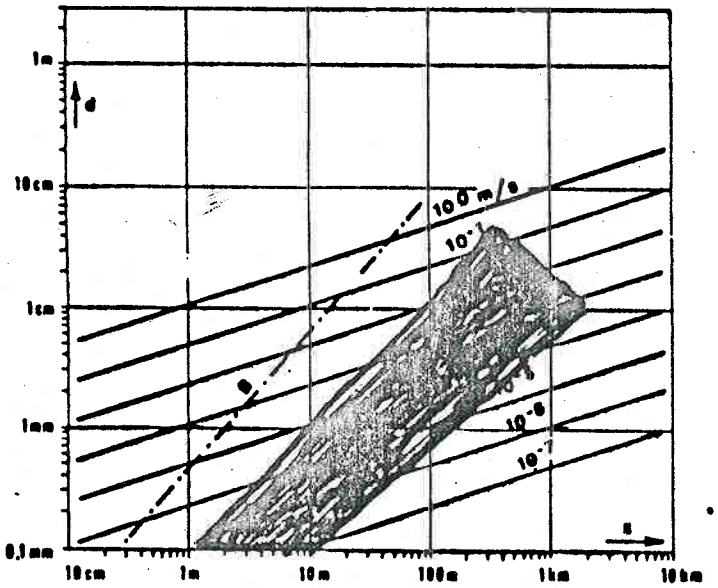

Fig. 22. — Effet d'échelle sur la perméabilité pour les réseaux de fissures.

d = aperture of fractures

KARST CHANNELS

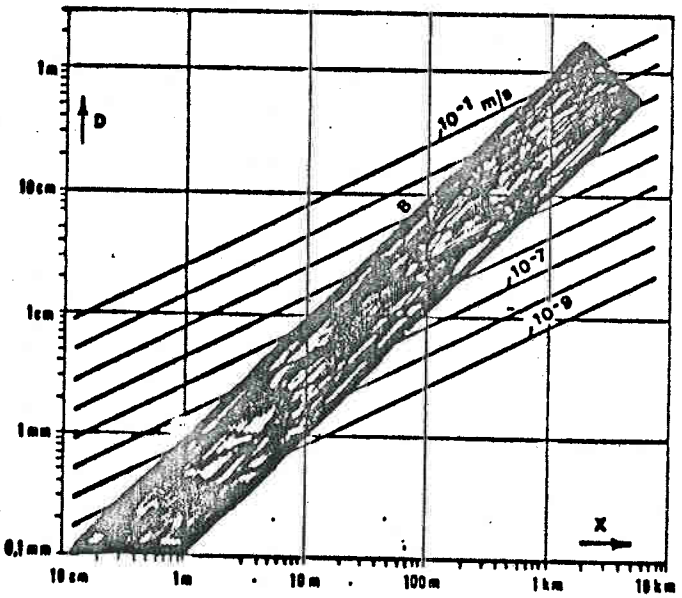

Fig. 23. — Effet d'échelle sur la perméabilité pour les réseaux de chenaux.

size of area considered

D = width of karst channels

SCALE EFFECT ON PERMEABILITY OF FRACTURED ROCK AND KARSTIFIED ROCK

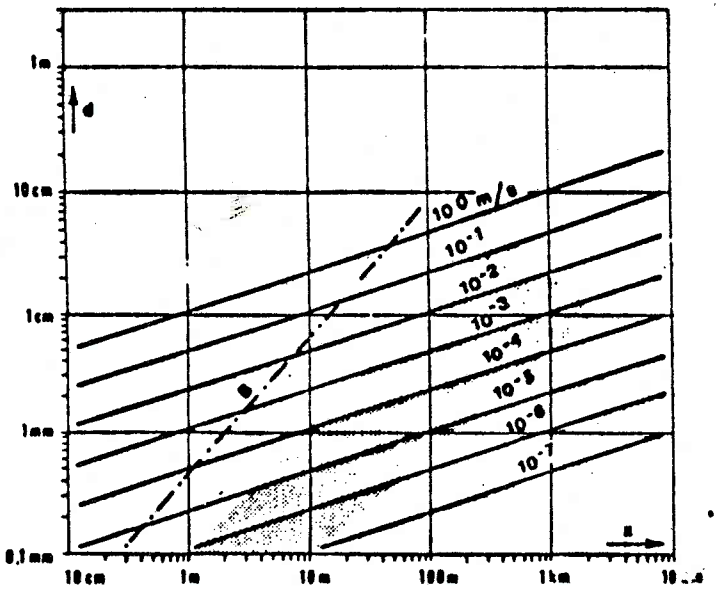

Fig. 22. — Effet d'échelle sur la perméabilité pour les réseaux de fissures.

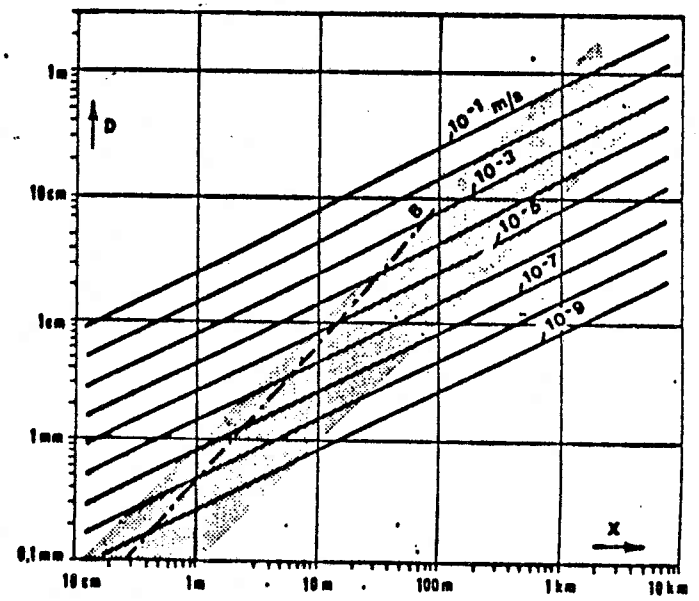

Fig. 23. — Effet d'échelle sur la perméabilité pour les réseaux de chenaux.

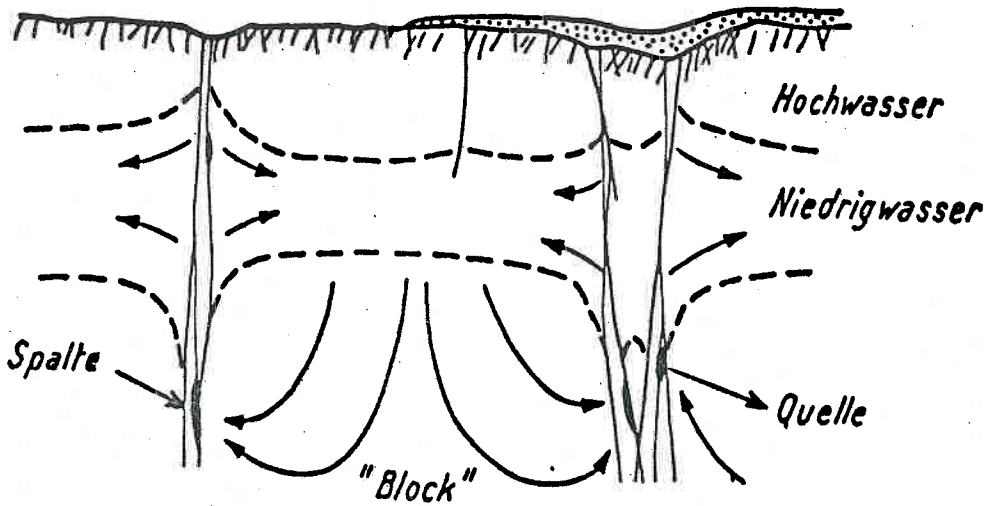

Fig. 11: Schema der unterirdischen Karstwasserzirkulation (nach A. Burger, 1979).

Burger, A. (1979): Recherche de critères pour la protection des eaux souterraines karstiques contre la pollution. Application au Jura suisse. Bull. Centre d'Hydrogéol. 3, 115–154.

SCALE EFFECT ON PERMEABILITY IN KARST

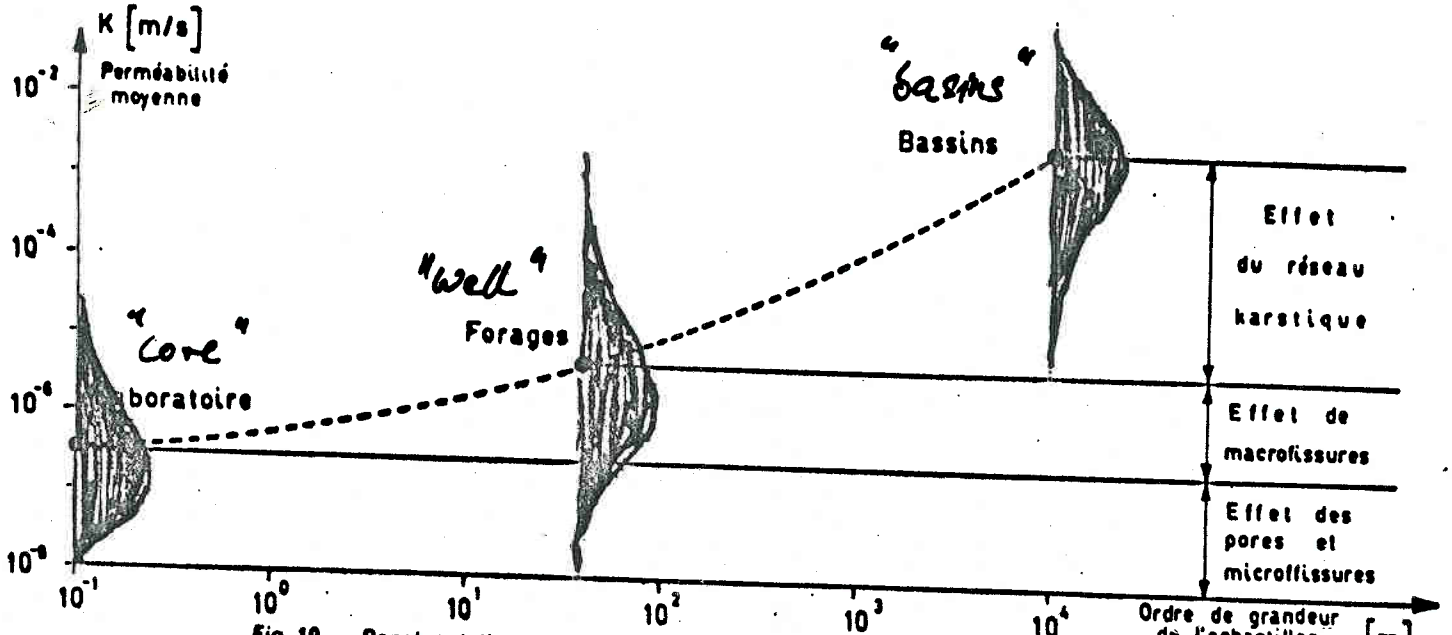

Fig. 19. — Représentation schématique de l'effet d'échelle sur la perméabilité dans le karst.

SCALE EFFECT ON PERMEABILITY IN KARST

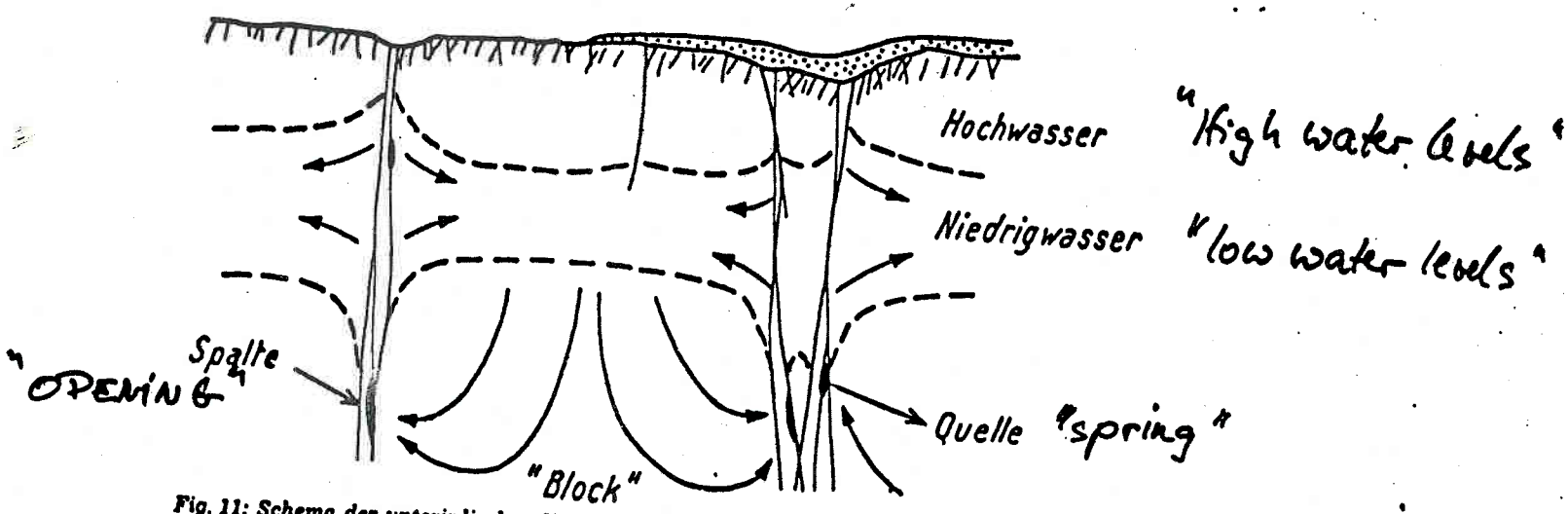

Fig. 11: Schema der unterirdischen Karstwasserzirkulation (nach A. BURGER, 1979).

BURGER, A. (1979): Recherche de critères pour la protection des eaux souterraines karstiques contre la pollution. Application au Jura suisse. Bull. Centre d'Hydrogéol. 3, 115–154.

SCHEMATIC DIAGRAM OF GROUND WATER FLOW IN KARST SYSTEMS (AFTER A. BURGER, UNIVERSITY OF NEUCHÂTEL, SUISSE)

Discuss Five Points

[illegible]

and possibly [illegible]

FIGURE 3-34

At the western end of the lake, elevated beach lines are at lower elevations as a result of differential changes in the elevation of the land due to postglacial isostatic readjustments of different magnitude (Cameron 1922a, p. 30; 1922b, p. 351-353; Raup, 1946, p. 28-30). The "slope" of westward tilting is slightly over 2 ft per mile (0.4 m/km; 0.04%; Craig, 1965, p. 18). Data from Andrew (1970), Prest (1968) and Mayewsky et al. (1981, Fig. 2.2) indicate that the Pine Point area has been unglaciated for about 10,000 years.

KARST DEVELOPMENT, COLLAPSE AND SOME ASSOCIATED DIAGENETIC CHANGES

BACKGROUND

In the past the nature of the karstic systems at Pine Point has been under-estimated as to extent and importance for present-day groundwater flow. For the purpose of dewatering it had been assumed that the cone of drawdown could be adequately predicted by means of methods developed for granular, non-karstic aquifers and that karst effects could be neglected (Vogwill, 1976). Karst development also has been considered as restricted to certain horizons and to the area of the Pine Point Barrier complex itself (Z. Nikos, personal communication, 1978; J. Collins, personal communication, 1980, K. Carter, personal communication, 1981).

The results of hydrogeochemical investigations lead Weyer (1978b, 1981 a, b; also presented in a talk at Pine Point Mines in September 1980) to conclude that karst systems in the Pine Point area are of regional extent. They spread not only along the Pine Point Barrier complex

but also towards the south; they are important conductors of groundwater at the site of orebodies and open pits; they continue to transmit considerable amounts of salt water and sulfate water towards the orebodies; and they extend towards much greater depth than previously assumed.

Only comment for Pine Point

Rhodes (1982,p. 10), in a recent paper observes that "it is worth noting that while published papers on Pine Point have mentioned karsting, it has never been given the prominance it deserves. In particular the interconnected and ramifying subhorizontal karst channels herein described are hardly mentioned in the published literature, though they are of major importance."

KARST FEATURES NEAR OREBODIES

'Normal', interconnected tabular and prismatic 'karsting'

"Most of Pine Point karsting occurs in a crudely strata-bound horizon coincident with the base of the Presqu'ile, which is itself coincident over much of the barrier complex with the base of the Sulphur Point Formation rocks [see Figure 3-35]. This association between Presqu'ile, karsting and mineralization results in two major trends of mineralization on the property coincident with the two main bands of Presqu'ile development on the east part of the property previously described. These two trends of karsting and ore development are referred to at present as the Main or North Trends or in Skall's [1975] paper as the Main and North Hinges". (Rhodes, 1982, p. 10, 11).

Karst development in the stratabound horizon is referred to as tabular karsting, while upwards extending collapse zones are called 'prismatic bodies' or, when mineralized, 'prismatic ore zones'. "In some ways the differentiation between tabular and prismatic orebodies is artifical since the amount of dissolution and collapse within, and subsequently above, various tabular ore runs varies from a few feet to the hundred plus feet of a prismatic body in a complete spectrum. The thickest collapse structures are however relatively rare and appear somewhat

randomly scattered. They have a roughly elliptical to ovoid surface plan suggesting they may be palaeosinkhole structures which formerly provided access for surface waters to the underground drainage system. Much of the mineralization in the prismatic orebodies is more intense than in the tabular ore zones, presumably because the prismatic collapse structures represented more effective and restricted traps for sulphides. The same ore textures are present in both tabular and prismatic orebodies although prismatic orebodies often show evidence of multiple phases of collapsing, brecciation and healing by internal sediments, sulphides and carbonate cements..... Waste contacts in prismatic orebodies are mainly geologically controlled by the edge of the collapse while ore/waste contacts in tabular ores tend to be a function of grade in more diffuse karst zones".

"Prismatic orebodies often show a zonation of lead to the top and centre of the collapse with zinc being enriched relatively toward the bottom; iron sulphides are also often best developed toward the top of collapse structures but tend to have deposited peripheral to the main mass of lead zinc mineralization. Variations in lead, zinc and iron content are evident in tabular zones but no systematic pattern or zonation has yet been identified." (ibid.,p. 13).

"It is evident from [normal type prismatic orebodies, like A-70] that substantial volumes of Watt Mountain Formation and Slave Point Formation have foundered and collapsed. This indicates that while the original karsting of the Pine Point Barrier may have initiated prior to Watt Mountain time, there must have been one or more subsequent episodes of karsting and possible rejuvenation of pre-existing channels to collapse this younger strata. Note that these collapses have their roots in tabular karst runs" (ibid., p. 12).

"This karsting is believed to have initiated during subaerial exposure and weathering of the barrier prior to Watt Mountain deposition, although it is possible that the karst processes may be of a kind associated with interfaces between fresh and saline water bodies in the subsurface" (ibid., p. 10).

The orebodies A-70, J-69, M-40, and K-77 belong to this group and have been inverstigated hydrogeochemically for this report (for position of orebodies see Fig. 5-1). At A-70 significant amounts of saline water are mixing with sulfate waters. The other pits show a dominance of sulfate waters. A detailed discussion of groundwater flow at open pits is given in Chapter 5.

Internal sediments

" The karsting at Pine Point has produced zones of variable cavity development from a rock with small interconnected openings resembling a sponge to larger more continuous caves and openings, now in large part filled with lithifield dolostones. These dolostones show fragmental or breccia textures as well as laminated, sometimes cross laminated, textures that are completely different from any of the original or presqu'ilized/dolomitized carbonates of the barrier complex. These dolostones are referred to at Pine Point as internal sediments and are believed to have been laid down in the karstic openings by subterranean streams and to have been derived from dissolution, crumbling, collapse and mechanical and fluvial erosion and transport of the original rocks." (Rhodes, 1982).

This report considers only unconsolidated (unlithified) sediments in cavities, vugs and fractures as "internal sediments" since most borehole logs submitted to the Mining Recorder had been "streamlined" beforehand and hence were void of observations of the above nature. The sediments considered for the computer aided evaluation were various types of mud, sand, pebbles and erratics. The regional occurrence of unconsolidated internal sediments is shown in Figure 3-36, as extracted from the available borehole logs.

Figure 3-36

'Isolated' prismatic karst features

"Apart from the interconnected tabular and prismatic karst features on the Main and North Trend which form one distinct palaeoaquifer system, there are two other karst situations evident on the property. One [system is related to] orebodies lying south of the Main Trend which are identical to the prismatic orebodies described but do not as yet have readily evident tabular karst horizons present. These bodies almost certainly are interconnected with karst systems whose channels are too small to have been detected by our drilling to date". (Rhodes, 1982, p. 14).

The orebodies R-61, T-58, and S-65 belong to this group and have been investigated hydrogeochemically for this report. No significant amount of salt water was pumped at these open pits; sulfate waters dominated. Groundwater flow towards R-61 was considerable causing delays in mining. Many of the pumps installed were positioned in a highly permeable SW-NE zone indicating groundwater flow from a southern direction. The drawdown at R-61 did not significantly affect water levels at the pit T-58 situated a comparatively short distance towards ESE. However, it exerted a significant drawdown effect at the comparatively distant open pit S-65 positioned towards the west approximately parallel with the direction of the North Trend and Main Trend.

"Anomalous", unconsolidated collapse features

"The other and more important karst derived features, separate from the previously described structures, are what have in the past been called sinkholes and thought of as being of more recent origin. For this discussion these structures are referred to as unconsolidated collapses. These collapse structures [illustrated in Figure 3-37] consist of poorly sorted grit to large boulder sized blocks of heterogeneous rock types, including sometimes glacial till within an unlithified sand to clay matrix.

FIGURE 3-37

"In contrast, the 'normal' prismatic bodies are composed of well lithified dolostones, internal sediments and collapse breccias and the collapse breccias,while often down-dropped considerably, maintain a semblance of the true stratigraphic order of the rocks. Some unconsolidated collapse structures appear to bottom at the usual tabular karst horizon; however, many penetrate very deep into the Pine Point Formation of the barrier and perhaps into the Keg River Formation, or even the Chinchaga Formation - composed predominantly of evaporites.

"In a number of instances unconsolidated collapses are mineralized; these include some of the major orebodies on the property such as X-15, W-17 and the A-55 orebody....These orebodies do not bottom out at the usual tabular ore horizon, rather they are found in areas where erosion has removed the normal prismatic and tabular ore hosting stratigraphy.

"In the case of A-55 [compare Figures 3-38, and 3-39 in this report] there appears to be the roots of a 'normal' prismatic orebody at surface. A later unconsolidated collapse appears to have stooped downward the upper part of a 'normal' prismatic orebody (i.e. mineralized Watt Mountain and Slave Point Formation as in A-70) and preserved this ore at depth. While much of the sulphide mineralization in these unconsolidated collapses appears to be mechanically derived clasts, there are within and peripheral to the collapses precipitated sulphide crystals and impregnation that indicate further chemical deposition of sulphides from solution after collapse [underlining inserted by this author].

FIGURE 3-38

FIGURE 3-39

"It is currently hypothesized that these unconsolidated collapses do represent younger collapse features than the 'normal' prismatic orebodies, though perhaps considerably older than the Pleistocene, that have their roots at one or more horizons where deep penetrating ground waters have dissolved limestones and/or evaporites. These deeper karst processes have often been localized by the same structural, lithologic and hydrologic controls as pre-existing "normal" tabular or prismatic karst features resulting in unconsolidated collapses 'rejuvenating' older karst bodies or occurring adjacent to older karst features. Where an unconsolidated collapse has occurred coincident with a prismatic orebody it may have produced an A-55 or X-15 situation." (ibid., p. 15, 16).

W-17 and A-55 have been investigated in detail hydrogeochemically for this study. In both cases saline and sulphurous groundwater occurred. At X-15 only three pumps provided auxiliary draw-down since the main draw-down was achieved by pumping the pit W-17. A very slight amount of NaCl was noted in the discharge from those three pumps. A detailed discussion of present groundwater flow conditions at open pits is given in Chapter 5.

An unconsolidated prismatic collapse orebody: A-55

The A-55 prismatic orebody is located in the North Trend. It has been described in detail by Alldrick (1982). The following descriptions have been extracted from his paper since it is not readily available. [square brackets indicate additions or modifications of the original text]. The deposit is the sixth largest lead-zinc ore zone on the Pine Point mining property totally 2.3 million tons at a grade of 2.4% Pb and 6.8% Zn.

Geological setting

The orebody is geologically located on the south edge of the North Trend belt of tabular and prismatic ore zones. The ore is hosted in a major

solution collapse structure that has developed through a regular stratigraphic succession (Figs. 3-38, and 3-39). The top of the orebody has been removed by glaciation and the collapse subcrops within host rocks of the Sulphur Point Formation.

"A sequence of low-displacement normal faults [is] exposed in the pit rim. While displacement on any one fault is in the order of two to three feet, the cumulative total over several of these faults is enough to maintain the same stratigraphic sequence exposed in the wall of the pit despite the low northward dips of about 8 degrees": (ibid., p. 3).

Collapse structure

"The orebody is hosted in a large diameter and unusually deep paleocollapse structure. At the 4th bench level [about 40 m below surface] the structure is elliptical in plan with the long axis oriented ENE-WSW along the trend of the barrier complex and measuring 400 feet by 250 feet [122 by 76 m]. At the 14th bench level [about 140 m below surface] the collapse narrows to 350 feet by 100 feet [107 by 30 m]. The deepest drill hole in the orebody area has intersected rotated, displaced blocks of recognizable Devonian lithofacies to the end-of-hole at 650 feet [198.1 m]. These blocks are unlithified and are undolomitized and unmineralized below 375 feet [114.3 m] in this hole. Since only one deep drill hole has been completed we have no data on the dimensions of this collapse below the 400 feet [122 m] level. Thus, the outline of the lowermost 250 feet of the collapse structure illustrated in Figure [3-39] is conceptual. The source bed for this collapse structure may be as deep as the Chinchaga evaporites.

"The upper level of the collapse structure is subdivided on the basis of the provenance of its fill. Most of the collapse is filled with angular blocks of Devonian lithofacies derived from the progressive upward stooping of the collapse through the barrier complex. This material and the portion of the collapse structure which it fills is termed 'paleocollapse' indicating that it developed between the Devonian Period and Pleistocene Epoch.

"In the upper three benches of the pit a large volume of the collapse structure is infilled with washed-in early Pleistocene age boulder clay and boulder beds composed of well-rounded cobbles of [various] lithologies such as granites, gneisses, amphibolites etc.. This Pleistocene debris-filled zone is termed [a] 'sinkhole' and most of the material shows evidence of [deposition in water]. This sinkhole material is clearly distinguishable from the overlying 60 feet thick blanket of buff coloured late Pleistocene till by its dark grey colour and its waterlain character. Clasts of Precambrian gneiss have been recovered in drill core [from] a depth of 365 feet [113.3 m, 13th bench] suggesting that the sinkhole fill may extend to at least the same depth as the ore mineralization" (ibid. p. 3, 4)

Alteration

" In the A-55 area, presqu'ilization has intensely altered the D2 facies rock and has less intensely altered the underlying B Reef Substrate lithofacies. In fact the degree of presqu'ilization of the B Reef Substrate unit can be seen to progressively decrease with depth in the A-55 pit walls."

"A critically important, albeit subtle, distinction can be made between the regional dolomitization effects of presqu'ilization and the massive intense dolospar replacement or veining which envelopes all the high-grade, collapse-hosted prismatic ore deposits. This latter type of dolomitization occurs as a halo around the main body of Pb-Zn-Fe sulphide ore and partially or totally replaces the original lithofacies, leaving no textural evidence of the original rock type.

"Although this massive dolospar replacement zone is a recognizable feature in all of the prismatic ore deposits, at A-55 it is sufficiently well delineated to be mappable. It is termed the 'Massive Alteration Halo' and the outer boundary of this zone is relatively sharp against the moderately presqu'ilized country rock and the inner edge is sharply defined by the paleocollapse structure. These sharp contacts suggest that this is a massive replacement of the country rock rather than a massive replacement of an early solution-collapse structure.

The orebody is enveloped by a second concentric, mappable alteration zone which is well-developed on the northern side of the paleo-collapse structure. This outer alteration zone is termed the 'Marcasite Impregnation Halo' and its distinctive feature is the overprinting of large discontinuous masses and pods of fine-grained greenish-yellow marcasite onto recognizable country-rock lithofacies" (ibid., p. 4).

Ore geology

"The ore at A-55 consists of sphalerite and galena with gangue minerals consisting of pyrite/marcasite, dolomite and calcite. The sphalerite may vary in colour from amber to dark, purple-brown to black in the coarse crystalline varieties, and from buff to dark brown in the fine-grained colloform varieties. The cadmium content of this sphalerite is too low to be recoverable.

"Galena typically occurs as coarse-grained, euhedral to subhedral aggregates, but rare examples of skeletal crystal forms have been recovered from other pits on the property. The silver content of galena at Pine Point is negligible.

"Iron sulphide occurs as coarse-grained brassy yellow pyrite aggregates or as fine-grained sooty black to greenish-yellow marcasite aggregates and impregnations. The iron sulphide is preferentially concentrated in the upper levels of the ore zone and extends laterally beyond the limits of the lead-zinc mineralization, into the host rocks, forming a mappable 'Marcasite Impregnation Halo' on the northern side of the orebody.

"Dolomite occurs as a massive coarsely crystalline white aggregate replacing the original material or as discrete coarse-grained dolospar veins. Where it has been deposited as open-space filling the exposed surface characteristically forms 'saddle shaped' crystals. Although typically white and opaque, translucent varieties and pink-tinted varieties have been noted at A-55. Blue-grey dolospar veins occur within the ore zone and in the peripheral 'Massive Alteration Halo'. The colour is due to fine, disseminated sulphide mineralization which is concentrated along the core of the vein.

"Calcite is a late-stage mineral at A-55 occurring as very coarse yellowish translucent 'dogstooth' spar, lining vugs and cavities. A minor number of narrow late-stage veins and veinlets host white sparry calcite.

"The outline of the ore in plan and in section is illustrated in Figures [3-38 and 3-39] respectively. The sulphide mineralization terminates abruptly with depth, but in the upper levels of the orebody minor lead-zinc sulphides occur laterally for a few tens of feet beyond the outline shown in Figure 3-38. Lead-zinc mineralization occurs both within the paleocollapse structure and within the massive alteration halo. Collapse-hosted mineralization occurs as clastic grains and blocks plus chemically remobilized pods and lenses of massive colloform sphalerite and coarsely crystalline galena. Within the alteration zone ore occurs as large irregular pods or blebs of massive , very coarse-grained sphalerite or galena. Fine grained black or greenish-yellow marcasite mineralization occurs discontinuously from within the paleocollapse structure to the outer alteration zone. In lower grade zones the sulphides may occur as cross-cutting veinlets or as disseminations in otherwise barren blocks within the collapse.

"Metal zoning within the orebody has not been established beyond noting that the Pb-Zn grade increases with depth and that the highest iron concentration is in the upper levels of the orebody" (ibid., p. 4,5).

The above description by Alldrick (1982) shows that gneissic sinkhole fill extends to at least the same depth as the ore mineralization but it does not become clear that the granitic and gneissic material is also imbedded in the orebody itself. Our investigation of borehole logs included boreholes from Conwest Exploration Company Limited which discovered the orebody and sold it to Pine Point Mines for mining. Conwest called this orebody the Anomaly 408. Descriptions of the following 22 boreholes were available to us: 408-1, 1a, 2 to 12, 12a, 13 to 20. Erratics were encountered in boreholes 408-9, 408-10, 408-12a, 408-14, 408-19 and 408 - 20. In several boreholes the erratics occurred clearly within the orebody.

In regard to ore distribution it is noteworthy that "lead-zinc mineralization occurs both within the paleocollapse structure and within the massive alteration halo" (Alldrick, 1982, p. 4). This alteration halo extends into the country rock. Black to greenish-yellow marcasite mineralization also occurs in fractures within the alteration halo.

Groundwater flow

At the time of Conwest's exploration (1966) groundwater was flowing through the orebody, most probably upwards. Flowing conditions were encountered at boreholes 408-2 and 408-3. The flow rate at borehole 408-3 was approximately 200 gallons/hour (∿ 0.3 1/s). Unfortunately no chemical data for this water are reported. A detailed discussion of present groundwater flow conditions near orebodies is found in Chapter 5.

Waterlevel responses to a pump test at the orebody A-55 revealed an additional important hydrogeological characteristic of karstic systems in the Pine Point area in general and near orebodies in particular, namely the plugging of karstic systems by internal sedimentation and the opening of such restricted karstic passage-ways by pumping stress (Weyer, 1981b). Figure 3-40 shows the corresponding temporary rebound of water levels in well hole 7 caused by the

---

FIGURE 3-40

---

associated increase in permeability. The natural occurrence of plugs in karstic channels of the area is important for the reduction of groundwater flow to open pits as proposed in Chapter 7. More detailed discussions are given there.

A tabular orebody: L-37

The orebody L-37 was the first tabular orebody to be mined by open pit methods, from 1979 to 1981. Ore reserves were 2.7 million tons of 1% lead and 3.9% zinc. The orebody is located on the Main Trend. It has been described in detail by Webb (1982). The following descriptions have been extracted from his paper since it also is not readily available.

Geological setting

The geological setting in the L-37 pit area is accentuated by "the occurrence of three recent (Pleistocene to recent) solution features termed sinkholes. These large, roughly circular features of undetermined depth are filled with black mud and Pleistocene glacial fill" (ibid., p. 2).

Sulphides occur as bedding replacement and open-space filling in porous dolomites, and as open-space filling within collapsed, solution channelways of a paleokarst system. These ore types combine to form an irregularly shaped, thin orebody that runs 3000 feet [915 m] along the 60° strike and, at its widest point, stretches 1200 feet [366 m] across strike. The maximum thickness of continuous ore grade material (greater than 2% combined lead and zinc) is less than 60 feet [18 m] and averages under 20 feet [6 m].

These dimensions, horizontally extensive and vertically restricted, typify a tabular orebody and distinguish it from the deep, roughly circular, collapse-controlled prismatic orebodies.

Ore geology

Lead and zinc mineralization occurs in three basic types that are specific to the host rock. Iron sulphide mineralization occurs intimately associated with these as well as by itself in the form of an iron sulphide layer. Together they make up the L-37 tabular orebody [see Figure 3-41].

FIGURE 3-41

The three main types are:

1) paleokarst solution channelway filling
2) stratabound bedding 'replacement' or open space filling, and
3) peripheral porosity infilling mineralization.

Two main *paleokarst solution channelways* occur within the pit, trending roughly 60°, coincident with the paleotopographic D2 buildup. Continuous paleo-collapses up to 100 feet [30 m] wide and 30 feet [9 m] deep can be traced for over 2000 feet [600 m]. Fine grained sulphides and white dolospar cement large fragments of surrounding dolomite. Sphalerite is the dominant sulphide mineral occurring as fine to medium-grained masses, and as colloform textures. Galena is less abundant and occurs as coarser-grained cubic and skeletal crystals. Fine iron sulphides, both marcasite and pyrite, are found throughout. These collapse-related ore zones are typically high grade, usually over 20% combined lead and zinc, often up to 50%.

Stratabound bedding 'replacement' is found in the southern portion of the pit within the well-bedded dolomitized H and I facies. In this case a specific bed, up to eight feet thick, is more or less 'replaced' by white dolospar and sulphides. Unaltered, this unit is a medium-grained cream coloured rhombic dolomite that has a finely bedded nature. Dolomitization, or presqu'ilization tends to accentuate this feature, creating a zebra-striped rock. Sulphides are associated with this alteration.

Upper and lower contacts are typically sharp for this ore type and represent the bedding contact. Horizontally, however, the contacts are gradational with sulphides grading rapidly into unmineralized dolomite. The overall effect is to produce a stratabound, erratic ore zone. Grades are quite variable, from nearly massive to trace sulphides, reflecting the degree of replacement.

Peripheral ore is often found in porosity adjacent to both previously discussed ore types. Types of porosity that have been mineralized include: a) fractures, particularly associated with collapse; b) 'moldic' porosity, common in the biohermal central region of the pit as well as within certain fossiliferous H and I beds; c) pin-point porosity from recrystallised rhombic dolomites within the H and I sequence; and d) portions of entire beds which for diagenetic reasons developed greater porosity preferentially.

In general, these peripheral ore types are irregular in outline and difficult to predict beyond the rudimentary association described. They do however add considerable thickness of primarily low-grade mineralization to the higher-grade collapse and stratabound ore types.

There appears to be a sulphide stratigraphy that has developed locally within the peripheral ore zones. A disseminated coarse-grained galena ore occurs highest up in the stratigraphy, with mixed sulphide ores occurring below. This mineralization sequence was observed in both collapse and stratabound ore types.

Capping the ore zones in the southern portion of the orebody, within the well-bedded H and I sequence of dolomites, there occurs a more or less continuous thin band of fine grained pyrite and marcasite. It caps the ore zones; no significant lead or zinc mineralization occurs above this layer. These cap sulphides form a band up to two feet [0.6 m] thick, with occasionally more diffuse infilling of adjacent porosity. The iron-sulphides are intimately associated with clays and fragments of C horizons suggesting that the iron-sulphides are replacing the clays trapped below the C horizons.

Lead and zinc mineralization occurs in the extensively presqu'ilized Sulphur Point Formation back reef and logoonal (H and I) facies of the Main Trend, roughly coincident with a palaeotopographic biohermal high (D2 facies). The L-37 orebody exhibits the characteristics of the tabular type, in being relatively thin (average thickness less

than 20 feet [6 m])and areally extensive. It is made up of mineralized palaeokarst solution channelways running adjacent to and within the biohermal unit, and a solution-thinned and replaced H and I bed that lies adjacent and to the south. Surrounding these ore occurrences are a variety of peripheral ores that spread out into local porosity. A galena type mineralization locally caps the ore zones. In the southern well-bedded H and I sequence, iron sulphides appear to replace clays along thin stratabound solution horizons, forming the highest sulphide occurrence.

The above description by Webb (1982) of the orebody L-37 contains one puzzling piece of information, the mixing of black mud and Pleistocene glacial material in the three Pleistocene (or Holocene) sinkholes associated with the orebody. Black mud has been encountered within our hydrochemical investigation in pumped waters at the open pits A-70, R-61, J-69 and W-17 and at natural discharge points downslope of A-70. It consisted mainly of iron sulphide, some of it forming presently at the discharge point, some of it obviously at greater depth.

From the above information it can be concluded that the black mud at L-37 has been deposited in the three sinkholes during or after their formation in Pleistocene or Holocene time. This indicates that groundwater from greater depth was precipitating ingredients of the ore zone in, geologically seen, recent time. These groundwaters would also have flown through the tabular orebody itself, as already suggested in Figure 3-41 by the connection between Pleistocene sinkhole and tabular orebody and the geometry in general. In this context it is interesting that, recently, banded lead zinc ore deposition has been found within the fluvio-glacial filling of sinkholes associated with orebodies at Pine Point (D. J. Alldrick, personal communication, 1982). Upward flow of groundwater would be a necessary prerequisite for formation of this kind of deposits. At A-55, and presumably in parts of most if not all other orebodies, upward flow of groundwater occurred before dewatering commenced in association with mining. The bio-chemistry of these waters (Weyer et al., 1979), under certain conditions, would have allowed precipitation of metal sulphides.

DEVELOPMENT OF KARST IN THE PINE POINT AREA

Background

Jennings (1971) has provided a nomenclature for sinkholes which will be useful for the discussions below. According to Jennings (1971) *solution sinkholes* are formed by solution from the surface down; *collapse sinkholes* are formed by shallow collapse of an underlying solution cavity; *subjacent karst collapse sinkholes* are formed by deep-seated collapse leading to breccia chimneys as a result of progressive upward stooping over the solution cavity; and *subsidence sinkholes* are created by gradual subsidence and flow of unconsolidated material into underlying solution openings.

In most papers published on the Pine Point area there seems to be an implicit assumption that karst structures in the area have been developed by dissolution from the surface down and hence constitute solution sinkholes in Jennings (1971) nomenclature. However, geologic and hydrogeologic results of the present investigation and a reinterpretation of published geologic data appear to support the view that most, if not all, karstic structures in the area have been caused by dissolution at depth and subsequent collapse, leading to collapse sinkholes and subjacent karst collapse sinkholes. In view of the occurrence of deeper seated saltwater at 'normal' prismatic orebodies interconnected with tabular karstification (orebody A-70), and at isolated prismatic orebodies (orebodies W-17 and A-15), subjacent karst collapse sinkholes are probably of major importance for the karst development in general and ore-precipitation and upward flowing groundwater in particular.

Karst development processes and their age.

Both the age of the ore and the age of the sinkholes are disputed. Kyle (1981, p. 730) stresses, that "there is no geologic evidence to indicate a precise age of mineralization during the 375 million years from the

Givetian to the present". While Webb (1982, p. 2) found clear evidence that Pleistocene or more recent sinkholes are associated with the L-32 tabular orebody, Rhodes (1982, p. 15) expressed reservations when stating "it is currently hypothesized that the(se) unconsolidated collapses do represent younger collapse features than the 'normal' prismatic orebodies, though perhaps considerably older than the Pleistocene, that have their roots at one or more horizons where deep penetrating ground waters have dissolved limestones and/or evaporites."

Devonian (?) paleokarst

Traditionally, karst development in the Pine Point area has been assumed to have started as solution karst from the surface down, usually in 'pre-late Givetian time' (Kyle, 1981, p. 678). Major parts of the so-called paleokarst are thought to have been formed at that time. Alldrick (1982) is of the opinion that the 'paleo-collapse' developed between the Devonian Period and Pleistocene Epoch. Because of the lack of direct geologic evidence, all of the proposed models in some way contain a speculative element.

Post-jurassic karst development

Post-jurassic salt dissolution at depth in the Mirage Point Formation lead to brecciation and fracturing of overlying rocks (Chinchaga Formation to Hay River Formation or even stratigraphically higher). During the solution process groundwaters became more saline and this increases the solubility for anhydrite, gypsum and carbonates (for details see Chapter 3, section 'Subsurface dissolution of carbonates and sulphates').

Because of mechanical and chemical reasons, salt dissolution appears to have been one of the strong promotors of karst development since Jurrasic time. The process of salt dissolution is presently still active. In Chapter 4 it will be shown that the various salt-solution breccias in

the Mirage Point Formation, the Chinchaga Formation, the various dolomite and limestone sequences and the Muskeg Formation, as well as deeper layers, and the Precambrian are still active parts of present-day groundwater flow systems. This condition may have existed since Jurassic time or even longer. Our data indicate that, on a regional scale, neither the Chinchaga nor the Muskeg evaporites (anhydrite, gypsum) are the barrier to groundwater flow they were intuitively conceived to be by many geologists. At the open pit W-17 saline water was pumped out of collapse structures in the Chinchaga Formation by the pumps 31, 33 and 34 (compare Fig. 5-14). Rhodes (1982, p. 14) also suspects that at Pine Point unconsolidated collapse structures may penetrate into the Chinchaga Formation.

Pleistocene karst development

Rapid, almost 'catastrophic', formation and possible rejuvenation of karst features occurred in the Pleistocene as a result of the repeated (20-30 times) advance and retreat of the Laurentide Ice Sheet. This is suggested by the relatively widespread occurrence of crystalline erratics within karst features in the Devonian bedrock in general (see Fig. 3-29B), by their occurrence within the A-55 orebody and below it down to 365 ft [111 m] depth, and by the occurrence of glacial till in sinkholes (for example, the three sinkholes associated with the orebody L-37).

Lake-level fluctuations of ancient Great Slave Lake (Lake McConnell after the last retreat) and previous interglacial lakes, as well as the influence of the ice sheet itself, exerted profound effects on groundwater flow directions and associated groundwater chemistry.

The chemistry must have fluctuated repeatedly between saline, sulphurous and fresh, with associated alternation of reducing and oxidizing conditions. The magnitude of chemical changes must have had a pronounced effect on precipitation and dissolution of secondary minerals such as $CaCO_3$, $CaMg(CO_3)_2$, PbS, ZnS and S° within the karst systems. Re-dissolution and re-precipitation must have occurred in response to changing chemical equilibrium conditions and solubility products in the multicomponent systems and still do. In some way it is surprising that no oxidizing phases have been reported

for the mineral paragenesis of the Pine Point ores. In fact, the mineral assembledges in the Pine Point orebodies seem to be simple PbS and ZnS accumulations with an unusual lack of other metals. One might compare this situation with the result of a repeated distillation process.

By now, oxidation of orebodies is known to take place close to the topographical surface in the domain of local, oxidized groundwater flow systems of carbonate chemistry. These flow systems originate in the overlying till and have penetrated higher level orebodies (like 0-42) for about 10 feet [3 m] and caused an oxidized, rusty appearance of the ore over about the same depth.

In the following a mechanism for the 'catastrophic' formation of karst-type features by the presence of an ice sheet is discussed.

Hydrodynamic blowout: a mechanism for 'catastrophic' creation and rejuventation of karstic features by the Laurentide Ice Sheet.

Hydrodynamic blowouts of groundwater in front of advancing or retreating ice sheets can be caused by water forces (potential gradients) created by the introduction of an elevated recharge area nearby (the ice surface). Hydrodynamic blowout structures result from water flow from a confined aquifer, through a discontinuity in the overlying confining beds. The process of groundwater discharge erodes a funnel-shaped elutriation cone, which eventually becomes partly filled with a breccia composed of particles too large to be expelled by the upward flowing water. A more or less cylindrical conduit extends from the aquifer up to the base of the cone (Christiansen et al., 1982).

Christiansen et al. (1982) tested this concept recently on Howe Lake in southeast Saskatchewan (Fig. 3-42). They showed convincingly that Howe Lake was caused by a hydrodynamic blowout in front of the Laurentide Ice Sheet.

FIGURE 3-42

Three hydrogeologic conditions are required for the generation of such a blowout (ibid., p. 1182): (1) the area must be underlain by an aquifer capable of delivering at least 0.04 m^3/sec; (2) hydrostatic pressure in the aquifer shall approach or even exceed the critical uplift or lithostatic pressure; and (3) a localized discontinuity must be present to initiate venting through the overlying beds.

Large pumping requirements at the pits of Pine Point Mines show that the first requirement is met. The second point is debatable because the forces are not determined by the pressure but by the gradient of the potential (Weyer, 1978a). In any case the second requirement would also have been met, because recharge was occurring through the ice sheet towards the east at higher topographic elevation and the connecting aquifer was of very high permeability. In fact the situation at Pine Point was probably more favorable than at Howe Lake, because karst structures usually have higher permeabilities than the Manville sand aquifer the permeability of which was estimated at $1 * 10^{-4}$ m/s by Christiansen et al. (1982). Hydrodynamic forces may have been aided by the generation of methane from hydrates which may have been present in front of the ice sheet. Warming of hydrates would have caused strong increases in gas pressure. Pockets of methane are now present in the Pine Point area (see Figure 3-53D) and, in one case reported, explosive discharge of methane lead to the scorching of the drill rig (Table 1.3: Hay River Test 6).

The requirements for an initial discontinuity is met by the carbonates which had certainly been fractured to some degree because of previous differential subsidence caused by salt solution. Also, older uncemented collapse breccias may have existed. Confinement would have been provided by the low matrix permeability of the carbonates, the overlying Hay River Formation or even by unconsolidated sediments.

Breccia-filled pipes ('sinkholes') have been described above in connection with the orebodies A-55 and L-37. The 'anomalous unconsolidated collapse features' are probably the remnants of hydrodynamic blowout events. The conducting aquifer may have been the Lower Keg dolomite or even deeper older permeable layers, which outcrop farther east. This would

explain the great depth of the unconsolidated collapse structures. Some of these 'collapse structures' contain important orebodies (A-55 and W-17).

LATERAL AND VERTICAL EXTENT OF KARST DEVELOPMENT

Background

The impressive extent of karst development within the Presqu'ile facies and other strata associated with the Pine Point Barrier Reef attracted exploration geologies working in this area to see this WSW-ENE oriented karst system as a constricted system of groundwater flow and associated ore genesis. Certain aspects of this concept were already challenged by Davidson (1966) and Roedder (1968a), who assumed groundwater flow from the south at the time of ore genesis, in association with the dissolution of the salt layers in the Elk Point Group (Muskeg equivalent; see Figure 3-21). More recently, Weyer et al. (1979) showed that currently regional flow systems carry saline and sulphurous groundwater from the Caribou Mountains in the south towards Pine Point in the north. This view has been disputed by some Pine Point geologists (J. Collins, K. Carter) who expressed the opinion that no significant karst could be found between the Pine Point Barrier and the known gypsum karst in Wood Buffalo National Park to the south, which had been investigated to some degree by Drake (1970) and Ford (1973).

After evaluation of data from approximately 1500 boreholes it is now possible to delineate the regional distribution of karst features both laterally and vertically. It will be seen that the carbonate rocks in the area could well be compared to a 'Swiss Cheese' with interconnected pores.

Interpretation of borehole data collected

It has been shown that karst systems and ore-mineral accumulations are intimately related. Hence the distribution of both ore-minerals and

porosity characteristics (cavities, vugs etc.) serve as indirect geological evidence in the assessment of the distribution of karst features.

Before considering the data in dependence of stratigraphic position, it needs to be recalled that the number of boreholes per stratigraphic layer is not constant but varies as shown in Figure 3-43. Note that

---

FIGURE 3-43

---

there are considerably fewer boreholes penetrating the Lower Keg (LA), Chinchaga (CH) and Mirage Point (MP) Formations. The Hay River (HR), Slave Point (SPF) and Watt Mountain (WM) Formations as well as the Pine Point Group (PPG) do not occur in the more eastern part of the map area. Also, some quite large areas on the Pine Point property and elsewhere are apparently devoid of boreholes. To the south of Pine Point there is a group of rotary-drill holes (Pine Point Swampy Lake Holes) of comparatively shallow depth providing much less information than the cored bore holes. Nevertheless, it will become obvious that the information collected allows valid conclusions as to the characteristics of the karst systems in the Pine Point area. The question of the respresentativeness of the borehole data has been discussed in Chapter 1.

Cavity systems are widespread in the Pine Point area and there is obviously no significant permeability impedance between the Pine Point Barrier complex and the gypsum karst in Wood Buffalo National Park (Figure 3-44). Cavities surprisingly occur in the Hay River Formation as well as in the Chinchaga Formation. Collapse structures, breccias and sinkholes occur regionally (Fig. 3-45). Again, these features seem to occur throughout the area, except for the sinkholes which, understandably, are not prominent in the area covered by Hay River shale. It should be noted that we tentatively identified more than one hundred additional sinkholes and blind sinkholes but could not list them in the computer files due to time constraints. Breccia occurrence are grossly under-

represented due to a late and incomplete inclusion into the computer listings. Brecciation does, however, occur from the Chinchaga Formation up to the Hay River Formation (Fig. 3-46) as was to be expected because of the salt solution effects described above.

FIGURE 3-44
FIGURE 3-45
FIGURE 3-46
FIGURE 3-47
FIGURE 3-48
FIGURE 3-49
FIGURE 3-50
FIGURE 3-51
FIGURE 3-52
FIGURE 3-53
FIGURE 3-54
FIGURE 3-55

The occurrence of vugs is widespread, both regionally and vertically (Fig. 3-47). One single occurrence of vugs has been reported for the Chinchaga Formation. The vugs in the area are not isolated as often presumed by exploration geologists, but are interconnected. They are often partially filled with minerals and hydrocarbons. Figure 3-48 shows the occurrence of additional widely interconnected porosity systems as *'spongy'* and *'very vuggy'* as well as *'pine point porosity'*. Again occurrence is regional, indicating one huge interconnected karst system.

For the properties *'broken'* and *'badly broken'* the same applies as for *'breccia'*; they are significantly under-represented in our computer files due to late and incomplete inclusion. Nevertheless, regional occurrence is clearly indicated, again presumably caused by the salt solution described earlier (Fig. 3-49). The resulting rock fabric would constitute an open crackle pack breccia (for definition see Table 3.1).

Internal sediments are widespread as well (Fig. 3-36). Off special interest to us is the occurrence of *green waxy mud* which was displaced downwards from the Watt Mountain Formation. This might be taken as an indication of downward flow of groundwater on one or more occasions in the past. The distribution of *black mud* also deserves attention as it

indicates the regional and continuing occurrence of mineral precipitation processes (see Chapter 4 and page 3.43).

Of prime interest are the occurrence of *sphalerite* and *galena* (Fig. 3-51) and ore accumulations and mineral showings (Fig. 3-50). It may be surprising to see these ore forming minerals occur over so wide an area, including areas to the south of Pine Point (Fig. 3-51). The formation of these minerals is intimately related to groundwater flow in karst systems. In a vertical sense we found these minerals occurring in the overburden, the Hay River Formation and all formations down to the Lower Keg Formation. They have not been encountered in the Chinchaga Formation or deeper in the stratigraphic sequence. The role of the Lower Keg dolomite as a regional aquifer will be discussed in Chapter 4.

Elemental sulphur occurs regionally as well (Fig. 3-52), and seems to be more widespread than assumed by Macqueen and Powell (1983). The formation of this mineral is also intimately related to flow and chemistry of water in karst.

Hydrocarbons occur within open voids in the rocks. They are also regionally widespread within the various strata and not associated only with the Pine Point Barrier as one might have assumed (Fig. 3-53, 3-54 and 3-55). Reported occurrence of methane is relatively widespread (Fig. 3-53D). Methane could have served as possible initiator of the hydrodynamic blowouts discussed earlier.

It should now be clear that large innerconnected karst systems with high porosities and hence permeabilities exist in the Pine Point area. These systems extend stratigraphically downwards at least into the Chinchaga evaporites.

The above computer evaluations confirmed the existance of a continuous regional aquifer system in the Givetian rocks of the Middle Devonian. It is comprised of the Slave Point Formation, the Watt Mountain Formation, the Pine Point Group (Sulphur Point Formation to the north, Presqu'ile and other facies in the Pine Point barrier complex, J-facies and Upper

Keg River Formation to the south) and Lower Keg River Formation. All these strata are strongly karstified. Although it is commonly assumed that extreme karstification is restricted to the area of the Pine Point barrier complex, it appeared from borehole logs of Giant Yellowknife (Appendix 2) that conditions of extreme karstification also exists between the barrier complex and Wood Buffalo National Park to the south. Cavities of up to 90 ft (about 30 m) were encountered during the exploration drilling. A thin layer of Presqu'ile facies also appears to extend into the area of the Wood Buffalo National Park.

Karstic collapse structures and tectonic structures provide for effective cross-formational flow through the Amco-shale, shaly parts of the Watt Mountain Formation, the Muskeg Formation, the E-shale and the Chinchaga Formation. Karst and other aquifer systems also exist below the Chinchaga Formation down into the Precambrian. These additional systems are dealt with further below (Chapter 4 and 5).

Chapter 4

remote permeability

Data Zarza oilfield ?// [illegible]
~~Dear~~ different from [illegible]
at [illegible] distance
[illegible]

4. REGIONAL GROUNDWATER FLOW

REGIONAL HYDRODYNAMICS

BACKGROUND

The principles of regional hydrodynamics have been described in Chapter 2. Regional groundwater flow is from the regional highlands towards the regional lowlands. Major rivers act as drains for deeper groundwater flow, forming hydrodynamic boundaries for the flow field. The situation in the study area is very similar to that shown in Figure 2-5. In the regional recharge area (Caribou Mountains) water penetrates downward into the Devonian aquifers (for geological cross-section compare Figure 3-7). From there it flows radially (compare Fig. 1-1) towards the forelands and discharge areas: Peace River to the south, Salt River and Slave River to the east, Little Buffalo and Slave River to the north-east, Great Slave Lake and the lower reach of the Buffalo River to the north, and Hay River to the northwest and west. From the viewpoint of regional hydrodynamics, the area is a natural laboratory with extraordinary topographical and geological clarity. It is mainly because of this reason that we were able to investigate the regional groundwater flow south of Great Slave Lake successfully with a minimum of technical installation (piezometers etc.) despite the vast extent (300 by 300 km) and inaccessability of the area.

OCCURRENCE OF ARTESIAN FLOW FROM BOREHOLES

In Chapter 2 it was shown that artesian discharge from boreholes only occurs in or close to natural discharge areas, when the head at a certain depth of the borehole is higher than the surface at the drill location, and the density of the water column in the borehole has not been increased by additives (drilling mud).

Use of mud additives is common practice in the oil industry, restricting water outbursts only to a few cases with exceptionally strong artesian conditions when occasional judgement errors are made. Companies are

required to record drilling histories in detail and submit them to governmental agencies.

In mineral exploration, drilling usually is done without mud additives and therefore artesian water flow is more common. The mineral exploration industry is, however, not required to submit detailed drilling information to government licensing agencies. For this reason, publicly accessible mineral exploration files contain information on artesian flow and its depth of origin only in exceptional cases. Nevertheless, the available information is sufficient to outline an accurate picture of the regional flow sytems as they existed before mining commenced.

FIGURE 4-1

Figure 4-1A shows that artesian flow from boreholes occurred in exactly the area where it was to be expected if the schematic diagram of Figure 2-5 were applicable to the region south of Great Slave Lake. The data on artesian conditions have been extracted from Table 1.3 for oil wells and from GEOBNK for mineral exploration holes.

RATE OF DISCHARGE AND IMPLIED HYDRODYNAMIC GRADIENTS

All oil wells drilled from the ice on Great Slave Lake (Hay River No. 1 I-41: Mid Lake H-33 and Sulphur Point No. 1 O-07) show strong artesian conditions with discharge of sulphurous and saline water. Discharge rates for Hay River No. 1 I-41 and Sulphur Point No. 1 O-07 were reported to increase considerably with depth, so that this condition, as well as shifting ice conditions, contributed to the abandonment of the holes, From the above data it is clear that the lake itself is discharge

area for the regional flow systems we consider here, as well as neighbouring systems originating in the Cameron Hills to the west and Horn Plateau to the northwest. Flow of water from the boreholes on the lake (6 and 23 1/s) and hence the permeabilities encountered prove to be high and need to be reckoned with in any estimation of the amount and areal extent of regional groundwater flow. It is also clear that flow directions are from the surrounding areas centripetally towards the lake and not parallel to its southshore as some earlier speculations assumed. The amount of groundwater flow and the associated permeabilities are also high in the adjacent area, south of Great Slave Lake, as documented by the drilling histories of a group of oil wells drilled close together inside one meander bend of the Hay River, about 18 km south of Great Slave Lake (Table 1.3: Hay River Test 1, 2, 3, 5B, 6 and 8; Fig. 3-3, position F; Fig. 4-2).

FIGURE 4-2

The first hole was drilled in 1922 by the Pure Oil Company in the valley bottom of the canyon of the Hay River; it led to a violent blow-out of water, delivering about 23 1/s through a 6.25 inch diameter hole 60 feet (18 m) into the air. In the judgement of the oil company it was the wildest blowout they had ever encountered (Pure Oil Company letter to G. S. Hume, G.S.C., 1942). In 1930, subsequent drilling near the river canyon by Atlas company, a subsidiary of Cominco Ltd., lead to artesian flows from both holes (Hay River Test 2 and 3), even though they were about 100 feet (30 m) above the valley bottom. At Hay River Test 3 the excess head was 15 feet (4.6 m) above surface. Hay River Test 2 was still flowing in October 1978 and sampled by us, as well as Hay River Test 5b. In both cases the water was sulphurous and saline. H_2S was found to be 200 mg/l in the water from Hay River Test 5B. Hay River Test 2 has ceased flowing since then.

Another indication for high fluid potentials and hence strong hydraulic gradients towards the lake is given by the flowing conditions encountered in Escarpment Lake No. 1 and Alexandra Falls B-07 (Fig. 3-3: EL; No.3).

Surface elevations at the drilling sites were 881 ft (268.5 m) and 730 ft (222.5 m) above MSL, respectively, indicating a head difference in the Slave Point Formation of more than 370 ft (112.8 m) between Escarpment Lake No. 1 and Great Slave Lake and more than 220 ft (67 m) between ALexandra Falls B-07 and the lake.

DEPTH OF ACTIVE GROUNDWATER FLOW

In the case of Alexandra Falls B-07, flowing conditions originated near the base of the Chinchaga Formation (Fig. 4-3), and delivered a brine with 183 g/l Cl^-, 4966 mg/l Ca^{2+} and 1631 mg/l Mg^{2+}. This fluid originates from the dissolution of Cold Lake Salt and is one of the agents for diagenetic processes as discussed in Chapter 3, further on in this Chapter and in Chapter 6. Let us recall that this brine is not flowing downdip towards the south (downdip flow of brine is often postulated because of increased fluid density), but it is flowing towards Great Slave Lake in the north, or the Hay River in the northwest.

FIGURE 4-3

The above discussions touched already upon the question of the existence of regional groundwater flow in strata below the Chinchaga Formation, and between and below salt layers in general. Intuitively many exploration and oil geologists tend to consider anhydrite and salt layers as locally and more importantly, regionally impermeable. While local impermeability or extremely low permeability may be defendable, permeability behaviour of regional anhydrite and salt layers is a different matter and needs to be evaluated in connection with the actually prevailing conditions. For the oil well Alexandra Falls B-07 we established already the existence of considerable groundwater flow below the Chinchaga evaporites. The records of the 1920 oil well Windy Point No. 1 by Imperial Oil (Fig. 3-3: WP) show artesian flow of salt water from the Mirage Point Formation, between Cold Lake salt and a deeper salt layer (Fig. 4-3). About 100 ft (30 m) above the top of the Precambrian, warm artesian water was encountered (Fig. 4-3).

Thus, strong evidence exists for active groundwater flow systems penetrating down to near the Precambrian. Below we will further strengthen the evidence with a discussion of the regional permeabilities of the different rocks encountered in the area.

INTERACTION BETWEEN GROUNDWATER AND SURFACE WATER FLOW

Weyer et al. (1979) reported the results of discharge measurements, taken along Buffalo River, Little Buffalo River, Nyarling River and Salt River, under low flow conditions during September 1977. These measurements and an additional one from Hanbury Creek are summarized in Figure 4-4.

FIGURE 4-4

The measurements were carried out by the Fort Smith Office of the Water Survey of Canada. Groundwater discharge is reflected in the measurements along the Salt River, Little Buffalo River and Nyarling River. As discussed in detail below, the high concentrations of sulphurous and saline components, and their increase in a downstream direction, indicated a large groundwater component for all three rivers. Groundwater discharge into the Salt River system in September 1977 was between 4 and 4.5 m^3/s ; it was somewhere between 3.5 and 4 m^3/s for the Little Buffalo River upstream of the confluence of the Nyarling River; it was about 1.5 m^3/s for the Nyarling River itself and zero discharge for Hanbury Creek. In the reach of the Little Buffalo River below the confluence of Nyarling River, no further groundwater inflow seemed to occur, based on the discharge of 5 m^3/s measured at the Resolution highway bridge. This measurement may not be very reliable, however, because low flow velocities were caused by an enlarged cross-section at this site. It is remarkable, nevertheless, that there was no flow in Hanbury Creek. Combined total groundwater discharge into Salt River, Little Buffalo River and Nyarling River in September 1977 was between 9 and 10 m^3/s.

Water of a different chemical composition was found in the Buffalo River upstream of Buffalo Lake. Discharge measurements as well as chemical considerations revealed that there was no significant inflow of deeper sulphurou and saline groundwater. Rather it seemed that the river was losing water, as the total flow upstream of Buffalo Lake diminished from 33.6 to 30 m^3/s (see Figure 4-4) despite the input from several small creeks. It may be that the river there recharges some water, through the Hay River shale, to the karst systems in the deeper subsurface.

Flow in the Buffalo River increased to 75 m^3/s below Buffalo Lake, due to other streams discharging into the lake. Just before the point where the river turns north, a measurement with 71 m^3/s indicated a loss of 4 m^3/s, while the next measurement downstream, with 76 m^3/s, indicated a subsequent gain of 5 m^3/s. This result appeared to be unusual. Checking the records of all respective discharge measurements it was clear, however, that no measurement errors had been made. We are now of the opinion that just upstream and in the area of the measurement of 71 m^3/s, a significant amount of river water is lost into the karst system, because the protective cover of the Hay River Shale disappears just upstream of this measurement site. From there this water would flow in a northerly direction towards the property of Westmin Resources and beyond. The water would probably flow along the NS structural elements found to exist close by (Chapter 3, section: Tectonics). We also suspect that in the area of the pronounced change in the direction of Buffalo River to the north, fresh groundwater may enter the river from the south. Part of this water may flow through a former stream bed of the ancient Buffalo River, which used to leave Buffalo Lake at its northeast corner, and joined the present stream bed in about this area. Weyer (1975) found a continuous river reach without bridging ice cover between there and a few miles upstream of the mouth of Buffalo River in November 1975, despite air temperatures as low as to -30°C; Buffalo River, Great Slave Lake and Mackenzie River were frozen over at the time (Fig. 4-5). Additional discharge measurements during 1980 were not conclusive because of the occurrence of a rain storm between measurements.

FIGURE 4-5

From where the Buffalo River turns north the river is cutting its bed deeper into the glacial till and, farther downstream, into the Devonian strata (compare Fig. 4-1). Before the river reaches the Pine Point highway, flow increased to 77.6 m^3/s. About a mile below the highway bridge the river enters the discharge area of regional, sulphurous, groundwater flow. There it is flowing above the Presqu'ile facies situated deeper in the subsurface (see Figs. 3-16 and 4-6). Sulphurous springs occur at its bank (Figure 4-7) as well as artesian boreholes.

FIGURE 4-6

FIGURE 4-7

The first of these boreholes and major springs are marked on Figures 3-16 and 5-1 as 'spring and borehole 104'. Discharge from both the spring and the borehole had ceased by September 1977. They were observed during summer 1978 by an automatic camera system. No further flow occurred.

At the mouth of Buffalo River, the flow seemed to have been reduced by about 0.5 m^3/s. This amount would be within the error of the measurement techniques used. It is, however, possible that at this time some water was recharged from the river into the Presqu'ile structure underneath. Additional discharge measurements during 1980 were not conclusive, because of the occurrence of a rain storm between measurements.

DISTRIBUTION OF RECHARGE AND DISCHARGE AREAS

From the above discussion of observed hydrodynamic features, and in view of the principles of regional groundwater flow, it is clear that

regional groundwater flow originates in the Caribou Mountains, penetrates downwards into the Devonian and older aquifer systems, and from there flows centrifugally towards the various regional discharge areas situated along the Peace River, Slave River, Salt River, Little Buffalo River, Nyarling River, the south shore of Great Slave Lake and the valley of the Hay River. Further regional recharge also occurs in the lowlands between Caribou Mountains and Great Slave Lake, in areas with elevations exceed 700 to 800 feet (215 to 240 m). Groundwater discharge maintains the swampy areas west of Little Buffalo River within Wood Buffalo National Park, and between Pine Point and the park boundary (see Fig. 4-8).

FIGURE 4-8

Local and intermediate recharge and discharge areas are superimposed on the regional flow systems.

REGIONAL HYDROCHEMISTRY

BACKGROUND

Figure 4-9 shows the regional distribution of the more than 600 water samples collected from boreholes, springs, rivers and lakes in the area between Peace River in the south and Great Slave Lake in the north. Methods of analyses have been described in Chapter 1.

FIGURE 4-9

Chemical and isotope analyses were used to finger-print the various groundwater flow systems. The geological setting described in Chapter 3 and its reflection in the chemistry of the groundwater, permit the use of hydrogeochemical methods to test the validity of the hydrodynamic model of regional and local groundwater flow outlined above.

In addition to detailed chemical analyses, sulphur and hydrogen isotope analyses were also conducted on about 500 of the water samples. It was felt that the hydrogen-isotope data would reflect the origin of the water, whereas the sulphur-isotope data would identify strata through which the water had moved.

Concerning sulphur isotopes it was known from earlier investigations in this area (Hitchon and Krouse, 1972; Sasaki and Krouse, 1969) that the $\delta^{34}S$ values in sulphates from Cretaceous strata (negative values down to -20°/₀₀) are distinctly different from $\delta^{34}S$ values in sulphates from Devonian strata (about + 20 °/₀₀). Since the major regional recharge area, the Caribou Mountains plateau, is comprised of Cretaceous formations whereas the surrounding lowlands to the east and north are composed of upper and middle Devonian strata, Weyer et al. (1979) showed that sulphur-isotope data were useful in delineating at least some of the groundwater flow patterns.

CHEMISTRY OF GROUNDWATERS

Major-ion chemistry

A comparison of the analytical results revealed three different types of water occurring in the lowlands (Fig. 4-10).

FIGURE 4-10

---

(1) a calcium-bicarbonate water, found locally in the glacial drift, (sample 33);

(2) a sulphate-bicarbonate water with Ca^{2+} as the main cation (with Ca^{2+} and SO_4^{2-} probably derived from Devonian gypsum layers; sample 95); and

(3) sodium chloride brines, presumably derived from Devonian evaporite layers (sample 146 is a brine with ∿ 25% TDS).

The chemistry of most of the other water samples seems to reflect mixing or evolution of these three basic water types, as illustrated by samples 100 and 157. Sample 191, in addition, documents the influence

of magnesium sulphate, originating either from the dissolution of the minerals carnallite, kieserite, epsomite and hexahydrite or a dedolomitization process with an associated generation of sulphate.

Diagrams of the results of all major ions analyses are shown in Figure 3-28.

The regional distribution of major ions in the groundwater reflects the regional hydrodynamic pattern (see Figs. 4-11, 4-12, and 4-13) and the respective recharge and discharge areas, as well as the vertical chemical zonation (compare also Fig. 4-8):

FIGURES 4-11
FIGURES 4-12
FIGURES 4-13

---

(1) bicarbonate waters in the glacial drift;
(2) $CaSO_4$ waters in the upper parts of the Devonian sequence; and
(3) saline (NaCl) waters, often with higher contents of $CaSO_4$ in the deeper strata of Devonian and Precambrian age.

In the regional discharge areas, the waters from zones 2 and 3 come to the surfac That is why the chloride distribution (Fig. 4-11), the sulphate distribution (Fig. 4-12) and the Ca^{2+} distribution (Fig. 4-13) emphasize the ring of discharging waters along the edge of our study area. The discharge of salt water between Little Buffalo River and Slave River leads to an increased content of Na^+ in the poorly drained soils of the Grand Detour complex, in amounts sufficient to limit agricultural production (Pringle et al., 1975).

If this model is correct, we should also find saline and sulphurous waters beneath the regional recharge area (the Caribou Mountains) and between the regional recharge area and the regional discharge areas. We are able to do so within the limitations of the available data. Table 1.3 contains all hydrochemical data for oil wells in the area, available from government files and from Richmond (1965). Figure 4-14 shows that highly

saline waters are flowing in the deep Devonian aquifers below the Caribou Mountains (compare with Table 1.3 for geological position of water samples). There is no oil well information available for the area of Wood Buffalo National Park. North of the park only the records of Sulphur Point No. 1 0-07 contain hydrochemical analyses. Therefore we can only assess the existence of salt water flow (by using oil-well information) below the Caribou Mountains, west of the park, in the Hay River area, and to the north below the lake. Salt water is flowing from the Caribou Mountains towards Great Slave Lake. The dissolved salt is derived from dissolution of Cold Lake salt for the deeper layers, and from dissolution of Prairie Evaporite salt and possibly Black Creek salt below the Caribou Mountains for aquifers above the Chinchaga evaporites.

FIGURE 4-14

FIGURE 4-15

Figure 4-15 shows that there are also high amounts of SO_4^{2-} in the same aquifers, originating from the Fort Vermillion member of the Slave Point Formation, the Muskeg Formation within the Pine Point Group and from deeper anhydrite and gypsum layers. Near the NW corner of Figure 4-15 there is a zone of low SO_4^{2-} content but elevated NaCl content, which extends from the Cameron Hills northward toward Great Slave Lake, indicating a lack of sulphates in the strata penetrated by the groundwater.

In summary the patterns of major-ion chemistry clearly follow the hydrodynamic pattern discussed earlier.

Sulphur and hydrogen isotopes

The sulphur-isotope data for dissolved sulphate and sulphide are summarized in Figures 4-16 (A) and 4-17(A), as measured in the waters. In Fig. 4-16(B) and 4-17(B) the isotopic compositions of the initial SO_4^{2-} are based upon isotopic balance calculations using measured SO_4^{2-} and H_2S concentrations and $\delta^{34}S$ values for sulphate and sulphide. These calculations used the following equations

$$F = \frac{[H_2S] \times 0.941}{[SO_4^{2-}] \times 0.334 + [H_2S] \times 0.941} \quad (1)$$

$$\delta S_{init} = \delta S_{SO_4^{2-}} \times (1 - F) + \delta S_{H_2S} \times F \quad (2)$$

where F = fraction of SO_4^{2-} reduced.
The constants in Eq. (1) are atomic weight ratios to convert ionic concentrations to sulphur equivalents.

FIGURE 4-16

FIGURE 4-17

In these calculations it is assumed that a closed system exists. If all sulphides were derived from sulphate reduction, the calculated values would represent the initial sulphate.

Based on the value of F determined in Eq. (1), the correct sulphur-isotope value δS_{init} is calcualted in Eq. (2). The calculated initial concentrations of SO_4^{2-} and the apparent initial isotope values for SO_4^{2-}, δS_{init}, were then plotted in Figures 4-16(B) and 4-17(B).

In Figure 4-16(B) the areas without stripes comprise sites where determination of $\delta^{34}S$ values for sulphide ions was not possible. Those entries are based on sulphate only; corrections for the presence of any sulphide would shift the majority to lower $\delta^{34}S$ values. Such corrections would further emphasize the three peaks in the distribution, with $\delta^{34}S$ values near +18.5, +9.5, and just below 0°/₀₀. Thus the isotopic-balance calculations restructure the data and permit the characterization of different water groups, as discussed later.

The question arose whether the isotopic differences between dissolved sulphate and sulphide reflect biological sulphate reduction or isotopic exchange processes such as

$$H_2{}^{34}S + {}^{32}SO_4{}^{2-} \underset{\leftarrow}{\overset{K}{\rightleftharpoons}} H_2{}^{32}S + {}^{34}SO_4{}^{2-}$$

Weyer et al. (1979) preferred the former interpretation for four reasons:

(1) the $\delta^{34}S$ value of the sulphate increases with increasing ratio of sulphide to sulphate concentration, consistent with kinetic isotope effects during sulphate reduction;

(2) their Figure 6 showed that the isotopic fractionation is not a simple function of temperature as would be the case in an exchange reaction where the equilibrium constant usually has a temperature dependance of the form $K \propto \ell n\ T^{-2}$;

(3) measured E_h values, consistent with a reducing environment seem to indicate sulphate reduction;

(4) general environmental conditions would not preclude microbiological activity.

Weyer et al. (1979) found that high isotopic selectivities associated with biological reduction significantly alter the $\delta^{34}S$ values of $SO_4{}^{2-}$ in waters of the area, even for relatively low percentages of reduction. Under these conditions chemical concentration data for dissolved sulphate, sulphides, and possibly sulphur compounds in intermediate valence states are necessary to identify the source of the sulphur species using $\delta^{34}S$ in $SO_4{}^{2-}$. The scatter diagrams in Figure 4-17 display the measured (A) and corrected (B) relationship between $SO_4{}^{2-}$ contents of the water and the $\delta^{34}S$ values for $SO_4{}^{2-}$.

Figure 4-17A shows $\delta^{34}S$ values of -10°/₀₀ and lower for the Cretaceous as previously reported (Hitchon and Krouse, 1972: Squares in Fig. 4-17A) and measured in this study (dots and triangle). The triangle in Figure 4-17A represents the value for a spring discharging at Fort Smith on the bank of the Slave River.

Isotope values in sulphate in waters from Devonian strata are clustered between +15 and +25°/₀₀. In Figure 4-17 (A) the majority of the waters from three different open pits cluster at the number 50 (signifying 50 dots not plotted).

Surprising is the occurrence of the single datum point 0°/₀₀ (diamond-shaped symbol). This value belongs to sample 191. We found it difficult to explain its occurrence before we made the correction for Figure 4-17(B). There the position of the point representing sample 191 becomes less anomalous, because the corrections cause seven other data points to shift into its vicinity. The probable reason that the $\delta^{34}S$ value for sample 191 was not shifted during the correction process is that the relatively high Hg-content of the water severly curbed H_2S production.

In general, the massive concentration of "Devonian" data points at number 50 in Figure 4-17(A) has been split into two groupings in Figure 4-17(B), one at number 26 (around +18°/₀₀) and the second one shifted to lower $\delta^{34}S$ values (around +10°/₀₀). The value for one spring (sample 192) which is located only some 20 m from the source of sample 191, did not shift to near the value for sample 191 in Fig. 4-17(B) after isotopic correction, but remained in the cluster near +18°/₀₀.

From the corrected results it appears that we are dealing with four different sources of sulphate, with $\delta^{34}S$ values grouped around the following values: -10, 0, +10, +18°/₀₀. The two extreme values are related to Cretaceous and Devonian sulphates, respectively. We suspect that the values of ∿ +10°/₀₀ might also be derived from Devonian strata while the values near 0°/₀₀ are suggestive of Cretaceous strata or some other unknown source. The intermediate values could also represent mixing of waters or a solution-precipitation-solution sequence.

The range of the $\delta^{2}H$ values obtained in this study (from -111 to -205°/₀₀ SMOW) indicates that the hydrodynamic systems in the area convey meteoric water. Figure 4-18 shows a plot of $\delta^{2}H$ values versus chloride (Fig. 4-18A) concentration for individual samples and versus topographical elevation of the sampling site (Fig. 4-18B). No obvious relationship exists between

---

FIGURE 4-18

---

the δ^2H values and the chloride concentrations on the one hand and the δ^2H values and topographic elevation of the sampling site on the other hand. A dependance on the topographical elevation could have been expected because differences in mean annual air temperature should be associated with elevation differences of more than 2000 ft (600 m) in the study area. The temperature differences in turn should be reflected in the δ^2H values.

Figure 4-18 also shows that the population of δ^2H values have a bimodal distribution with peak one at about -135°/₀₀ and peak two at -170 °/₀₀. Samples associated with peak 1 come from springs, lakes and rivers with dominant surface water or shallow groundwater component (Mackenzie River, Buffalo River, and the karst spring in the canyon of the Little Buffalo River near the road to Fort Smith - Sample 148). Samples associated with peak 2 come from sulphurous karst springs and boreholes (Angus Tower Spring, Halfway Spring, boreholes at open pits, as W-17 and R-61). The regional distribution of samples belonging to group 2 is shown in Figure 4-19. Groundwaters from group 2 are only found

---

FIGURE 4-19

---

in the regional discharge areas of sulphurous and saline groundwaters. The bimodal distribution of the δ^2H values (Fig. 4-18) reflects the climatological conditions under which the water has been condensated. Hence, water samples in group 1 have been recharged from rain, water samples in group 2 have been recharged from melting snow and ice.

CHEMISTRY OF SURFACE WATERS

Major ion chemistry

In the regional discharge areas the chemistry of surface waters is affected by admixture of sulphurous and saline groundwater (Fig. 4-20).

FIGURE 4-20

This is less obvious in the Buffalo River which flows through the pronounced regional discharge area for only about 20 km and has a high

flow volume, whereas the Little Buffalo River flows through regional discharge areas for more than 250 km while its flow volume is comparatively small. The canyon of the Hay River is underlain by Hay River shale, and flow in this river is usually even more substantial than that in the Buffalo River. Hence, the chemical composition of its water is not very substantially affected. Nyarling River, other than during storm-flow and snow melt periods, carries a very high proportion of groundwater as indicated by its water chemistry. The same is true for the Salt River. A dilution effect observed in the lower reach of this river is probably due to a gain of fresh water. This had already been observed by Camsell (1917).

Table 4.1 lists changes over time in the chemistry of three of these rivers close to their confluence with Great Slave Lake. For the Little Buffalo River there appears to be a relative lack of Cl^- and also SO_4^{2-} in the measurements for 1976 and 1977. In 1960 and from 1979 onwards, the saline component in the water appears to be much more pronounced. An explanation for the observed conditions will be given in Chapter 5.

FIGURE 4-21

Isotope chemistry

Sulphur-isotope data for river waters also show characteristic trends (compare Fig. 4-21). In view of our discussions above, Little Buffalo River, Nyarling River and Salt River are clearly dominated by groundwater which has penetrated Devonian rocks. All other rivers studied are more or less affected by water with Cretaceous sulphur isotopes. In September 1977 the Buffalo River showed some effect of Devonian sulphate although its sulphate concentration was lower than in 1976. We believe that in 1977 the source of the sulphate was from Devonian rocks contained in the glacial till while in 1976 there may have been a stronger influence of groundwater from Cretaceous rocks.

PERMEABILITY OF ROCKS

BACKGROUND

Porosity and permeability of the carbonates in the Pine Point area have been discussed earlier with respect to the extent of karst development. It was shown that karst development is widespread in the Middle Devonian carbonate layers above the Chinchaga Formation in the Great Slave Lake area. It is further suspected that the determination of permeabilities or transmissivities through pump tests is inadequate because the evaluation methods used are not suitable for karstic rocks. In addition, it has been shown that pumping stresses can progressively increase the permeability by cleaning of karst cavity systems (compare Fig. 3-40).

Finally, anhydritic and gypsiferous layers within the Fort Vermillion member of the Slave Point Formation, the Muskeg Formation and the Chinchaga Formation were not considered to be a significant hindrance for groundwater flow, on a regional scale.

MEASUREMENT OF PERMEABILITIES

Before proceeding with more detailed discussions the Tables 4.2 and 4.3 are introduced to enable the reader to make a comparison between the various transmissivity units (Table 4.2) and coefficients of permeability (Table 4.3) cited. Conversions given in Table 4.2 are merely a function of differing units used to calculate the transmissivity. Table 4.3 lists the three basic definitions for the coefficient of permeability. The hydraulic conductivity K is derived from Darcy's (1856) experiment; it lumps together all constants related to the properties of the rock, the fluid and the force vector. The energetic treatment by Hubbert (1940) leads to the fluid conductivity σ lumping together the properties of the penetrated medium and the fluid. In the petroleum industry the intrinsic permeability k is in use which refers only to the geometric properties of the medium. Simple conversion factors between these parameters cannot be given because those factors are dependant on density and viscosity (temperature). The ranges of measured groundwater temperature (from 2°C to > + 40°) and density (from 1.0 to > 1.2 g/cm^3) are sufficient

to change permeabilities by more than 50% for the same medium. Therefore conversions should be done for each set of values separately.

PERMEABILITY OF MIDDLE DEVONIAN CARBONATES

Field values reported for the Pine Point Barrier

Results of field permeability and transmissivity determinations from pumptests are provided in Table 4.4 of this report. The field values were determined using pumptests. Pumptest theory has been developed for granular aquifers. Application of pumptest theory to highly fractured and karstified rocks at Pine Point may lead to questionable results.

Vogwill (1976)reported transmissivities near orebodies in the range of 0.005-0.03 m^2/s (Table 4.4). Golder Associates (1979, 1980) determined hyraulic conductivities in the range of $4 * 10^{-3} - 1.6 * 10^{0}$ cm/s and transmissivities from 0.02 to 0.172 m^2/s for Westmin Resources'orebodies X-25 and R-190. At the orebody R-190, very high transmissivities were determined as follows (Golder Associates, 1980):

Calculated median:	0.125 m^2/s
Watt Mountain/Slave Point:	0.00245 m^2/s
Upper Presqu'ile:	0.172 m^2/s
Lower Presqu'ile:	0.102 m^2/s

An additional pumptest led to a lower but still very high transmissivity value. At the Pine Point orebody T-58 an average transmissivity of 0.011 m^2/s was determined by Hills (1977). Hoffman (1980) determined an average transmissivity of 0.019 m^2/s for the orebody K-77.

For the Pine Point well site Legette et al. (1968) determined a transmissivity of 0.027 m^2/s. These values show that field permeabilities and transmissivities reported for the carbonates of the Pine Point Barrier are high.

Permeability of vugs

Cores from the oil well CDR Wood Buffalo C-74 were inspected for vugs. Flow through vugs penetrating the core was measured (Table 4.5) at a depth of 893.6 ft or 263 m (Fig. 4-22A), 930.1 ft or 283.5 m

(Fig. 4-22B), 959.8 ft or 292.5 m (Fig. 4-22C), and at 971.6 ft or 296.1 m (Fig. 4-22D). The Figures illustrate the appearance of the vugs. They are not the isolated type created by limited fossil dissolution.

FIGURES 4-22 A, B, C, D

The cores were taken from the Pine Point Group (UA) and the Lower Keg River Formation (LA). Flow rates through the vugs are substantial, coming close to 1000 m^3/year for some of the vugs of limited dimensions. From this it is clear that very substantial amounts of groundwater can circulate in the vuggy permeability systems alone, especially within the Upper and Lower Keg Formation, one of the regional aquifer systems.

Intergranular permeability of carbonates

Porosities and intergranular permeabilities were determined on cores from several oil wells and exploration holes (summarized in Table 4.6). Some of the porosities were surprisingly high, ranging from 1.5 to 23.6 °/o (see Figure 4-23 and Table 4.6). Sedimentological characteristics of cores tested in the permeameter are given in Appendix 3 under CDR Wood Buffalo C-74. The range of permeabilities in carbonates was from $3.3 * 10^{-5}$ to $1.3 * 10^{-9}$ cm/s for water and from $1.19 * 10^{-5}$ to $2.31 * 10^{-9}$ cm/s for air. In the carbonate rocks tested, intergranular permeability is of secondary importance as compared to karstic, vuggy and fracture permeability.

PERMEABILITIES OF ANHYDRITE AND GYPSUM LAYERS

Karstic systems

It is commonly assumed that anhydrite and gypsum layers are impermeable or nearly so. Figure 3-10 for example, taken from Skall (1975) gives the impression that the anhydrite layers of the Muskeg Formation south of Pine Point act as a barrier to groundwater flow. Since Skall's (1975) publication this opinion is widespread in relation to the groundwater flow south of Pine Point. We have already seen that karstic systems in this

area penetrate into the Muskeg Formation with its sandwich layer system anhydrite-dolomite. Salt dissolution caused breakage of overlying dolomite and anhydrite layers, with gypsum healing fractures in the anhydrite layers. The occurrences of unfilled fractures, of gypsum-filled fractures, of collapse structures and breccias, of internal sediments (sand and mud), and of vugs in the Muskeg Formation (Fig. 4-24) serve as indications that karstic systems penetrate the Muskeg Formation. Skall's choice of CDR Wood Buffalo C-74 for his regional geological cross-section was unfortunate in so far as the core-recovery rate of more than 90% was significantly higher than the recovery rate in the neighboring CDR Wood Buffalo L-42 and C-03A (63 and 57% respectively). Both latter boreholes are full of cavities in the Devonian strata, including the Muskeg Formation (Compare Appendix 3, Hydrogeologic evaluation of CDR Wood Buffalo C-74 and L-42)

Open fractures within anhydrite layers

Most fractures within anhydrite layers are now filled with gypsum. In response to changing chemical characteristic of the groundwater -evidently caused by changing hydrodynamic flow patters since the last glaciation - dissolution of gypsum along these fractures is ongoing, as are further diagenetic changes of anhydrite to gypsum. Both processes will allow us to identify groundwater flow in anhydrite layers in the area.

The permeability of a gypsum filled fracture was determined with $1.3 * 10^{-8}$ cm/s from air testing and $7.7 * 10^{-9}$ cm/s from water testing (Table 4.6, C-74: depth 288.7 ft or 88 m). During testing it was observed that fresh water would dissolve and erode the gypsum very readily along slight grooves, edges etc. An inspection of the core from CDR Wood Buffalo L-42 identified open fractures where the gypsum had been dissolved (Fig. 4-25). Passageways had been opened through the gypsum in the oblique fractures. Dissolution and evidence of groundwater flow was also found in horizontal fractures in the same core (Fig. 4-26). X-ray diffraction analyses (Appendix 3, CDR Wood Buffalo L-42) showed

that gypsum and anhydrite were present on the horizontal fracture, and that gypsum, anhydrite, dolomite and a trace of quartz were present along the opening in the oblique fractures. Flow tests of the openings in the oblique fractures (Table 4, 5, L-42) indicated a flow of about 200 m^3/year through the one opening and about 900 m^3/year through the other. During testing, the openings were enlarged by dissolution, leading to a gradually increasing through-flow. We are confident that such openings are part of an interconnected network penetrating the anhydrite layers, because of the mere fact of their occurrence and because of the deposition of dolomite found in some of the openings.

Our findings are supported by the investigation of an additional piece of anhydritic core from CDR Wood Buffalo L-42 in 534 ft (163 m) depth in the Muskeg Formation (Figs. 4-27 to 4-30). Again we found dissolution of anhydrite and change into gypsum on horizontal fractures (Fig. 4-27). We also found roundish gypsum accumualtions (blebs) associated with fractures (Figs. 4-28 and 4-29). An infrared spectrometric analysis (G. P. Michael, ISPG) confirmed that the white blebs consist of gypsum, whereas the dark matrix of the core is anhydrite. The white blebs show a zonation of growth rings of gypsum (Fig. 4-30) consisting of layers of gypsum. In the vertical fracture, leading downwards toward the white blebs, salt was identified by taste and dissolution when washing the core and a subsequent precipitation of a rim of salt crystals when drying it (Fig. 4-29). The origin of the salt and its exact composition are not known sofar.

In summary it has been shown that south of Pine Point, groundwater can flow in appreciable amounts through the anhydrite layers of the Muskeg Formation, contrary to widespread opinion. There is no reason to assume that groundwater would not flow through the Chinchaga anhydrites as well. Hydrodynamic findings support this conclusion.

PERMEABILITY OF SALT-DISSOLUTION BRECCIA, GRANITE WASH AND BASEMENT ROCKS.

Groundwater has been flowing in great amounts through the salt solution breccia remnants of the Cold Lake salt. A deeper breccia caused circulation losses during drilling in the oil well [Iskut] Little Buffalo K-22 (see Table 1.3, sheet 2).

Determinations of the intergranular permeabilities of the granite wash and the crystalline basement showed high permeabilities of 4000 and 1.0 Millidarcy respectively (Table 4.5). Additional fracture permeability would cause an even higher bulk permeability. The highly saline waters present would dissolve rock material leading to an increase in permeability. On the Salt Flats near Forth Smith the roots of partially imbedded granitic boulders have been dissolved within 10 000 years by highly saline waters. Todate the remnants of the erratic boulders rest above ground with a flat, 'cut-off' surface on the Salt Flat (R. Stein, personal communication, 1982).

Re/Spec Ltd. (1983), investigating granitic stocks in a geothermal area in Montana, found that the stocks had high permeability on well interconnected fracture systems, conveying meteroric water. From kinetic calculations it was estimated that chemical alteration and dissolution of rock material by circulating non-saline groundwater of 85°C could increase fracture apertures by 6 mm in 10,000 years.

In summary, it appears that large amounts of groundwater can flow beneath the Chinchaga evaporites within the rocks of the Mirage Point Formation, the granite wash and within the gneissic and granitic basement rocks.

Chapter 5

Add

map dewatering
map 1968/69 flow
map 1983 flow + Capture zone
diagram flow at springs
etc.

revise pre-mining vs. mining situation

1. Even in 1983, after 15 years of strong pumping, regional groundwater flow still comes from the south and turns west toward Buffalo River and east in direction to the pumping A-55 open pit. In the area of the W85-N orebody water continues flowing north towards Great Slave Lake. Therefore it is proven that there is no water drawn along the barrier reef from areas farther west as postulated by the GTC report; also so far no water is drawn from the Buffalo River.

2. Drawdown in the Muskeg area towards the south of the barrier reef has been 25 to 30 feet between 1976 and 1983, as measured by Pine Point Mines at several piezometers.

3. South of the barrier reef there exists a groundwater "plateau" with low piezometric gradients pointing north, while relatively high S-N piezometric gradients exist within the barrier reef. North of the reef, not far from W85-N, an area of low gradients appears to exist.

4. Physical principle contained in Darcy's equation and the continuity equation dictate explanation for the situation described under 3 as follows:
   a. the permeability and transmissivity towards the south of the barrier reef is higher than the permeability and transmissivity within the barrier system itself, some areas towards the north also appear to have a higher permeability,
   b. Mechanisms effecting the permeabilities are
      - in the reef reduction of permeability and transmissivity by facies change and secondary diagenetic processes,
      - towards the south, in the gypsum and anhydrite layers of the Muskeg Formation and the layers nearby increase of permeability by dissolution and collapse Karst processes.

5. The concept of capture zone vs. total drawdown area shows that a preferred and directional effect of the pumping is exerted towards the south.

6. Pumping at the new pit N-81, situated in the southern part of the reef barrier, will exert strongly increased effects on the ground water flow in the area south of the barrier reef because
   a. there is a lack of a "buffer" of lower permeable reef material between the pit and the higher permeable area in the south,
   b. total depth of dewatering will be about 400 ft (from 710 ft to about 310 ft.),
   c. in all likelihood both factors above will create an unprecedented cone of depression of ground water levels estending much further south than presently.

7. In all likelihood the following scenario will occur:
   a. amount of groundwater pumped at N-81 will exceed significantly the predicted rate (2.8 m^3/sec) or planned depth of dewatering will not be achieved,
   b. costs of dewatering will seriously effect the profitability of the mining operation at N-81,
   c. the dewatering operation at N-81 will increase effects on groundwater flow in Wood Buffalo National Park. One cannot exclude effects on the nesting area of the whooping cranes, because during nesting season the swampy character of their nesting is sustained by discharge of ground water.

8. a. Flow from Great Slave Lake towards A-55 pumping is neglible if it exists at all (flow map, pump test, lack of drawdown at X-51 to X-56, dry holes, low permeability barrier).

   b. Drawdown map shows
      1. drawdown extends directional towards east and south (map based on relative high May, June 1983 water conditions; low pumping stress).
      2. water flow diverted away from X-15 and W-17 towards A-55.

A. Calculate T from dewatering rate

Here we assume that the dewatering at the open pit R-61 is essentially a long-term pumping test.

Use the steady-state equation:

$$Q = 2\pi T \frac{S}{\ell n\ (R/r_w)}$$

where: Q = pumping rate in m^3/day

T = transmissivity of the aquifer in m^2/day

S = drawdown in pumping well in m

R = radius of influence in m

r_w = radius of pit in m

Take: $Q = 7 \times 10^4\ m^3$/day

S = 110 feet = 35 m

R = 10 km (not a sensitive parameter)

(a) r_w = 300 m

$$T = \frac{Q \ln(R/r_w)}{2\pi S}$$

$$= \frac{(7 \times 10^4) \ln\ (10^4/300)}{2\pi\ (35)}$$

$$= 1100\ m^2/day$$

$$= 10^{-2}\ m^2/sec$$

(b) r_w = 30 m

$T = 1850\ m^2/day = 2 \times 10^{-2}\ m^2/sec.$

NB: T not very sensitive to r_w

B. Calculate drawdown at 25 km with T = 1850 m^2/day

Q = 7 x 10^4 m^3/day, using this equation:

$$S = \frac{Q}{4\pi T} W(u)$$

$$u = \frac{r^2 s}{4Tt}$$

where

S = the drawdown in m measured in a piezometer at a distance r in m from the pumped well

Q = the constant well discharge in m^3/day

s = the dimensionless coefficient of storage

T = the transmissivity of the aquifer in m^2/day

t = the time in days since pumping started

$$W(u) = -0.5772 - \ln u + u - \frac{u^2}{2.2!} + \frac{u^3}{3.3!} - \frac{u^4}{4.4!} + \cdots\cdots$$

(a) Take: s = 0.001, t = 60 days

$$u = \frac{(25{,}000)^2 (.001)}{(4)(1850)(60)} = 1.4$$

$W(u) \simeq 0.11$

$$S = \frac{(7 \times 10^4)(0.11)}{(4\pi)(1850)} = 0.33 \text{ m}$$

(b) Take: s = 0.005 t = 60 days

u = 7.04

$W(u) \simeq 8 \times 10^{-5}$

S = 0.00024 = 0.24 mm

(c) Take: s = 0.0005, t = 60 days

u = 0.7

$W(u) \simeq 0.4$

S = 1.20 m

Conclusion: Based on a dewatering rate of 7 x 10^4 m^3/day and a drawdown of 35 m, the transmissivity is about 1850 m^3/day and drawdown at 25 km distance could be between 0.33 and 1.2 m after 60 days. Reversal of drawdown (recovery) would be similar.

Fluctuations of water level elevations in the spring pond at Angus Tower.

	1981				1982	1983
	June 4[2]	Aug. 13	Sept. 22	Oct. 18	Aug. 7	Oct. 13
Overflow [m]	98.011	97.991	97.984	97.994	97.837	
Spring pond water level [m]	97.467	97.480	97.390	97.372	96.865	
Difference datum[1] to water level [m]	2.533	2.520	2.610	2.628	3.135	
Difference datum[1] to overflow [m]	0.544	0.511	0.594	0.622	0.972	

1) datum assumed to be 100 m.

2) differential movements of about 0.5 m noticed between the two ends of the chain of spring ponds.

FLUCTUATIONS OF WATER LEVEL ELEVATIONS IN THE SPRING POND AT ANGUS TOWER.

Distance from Halfwaysprings			
A 70	-	32.5 km	13 cm
A 55	-	31.2 km	12.5 cm
R 61	-	23.74 km	9.5 cm
N 81	-	30 km	12 cm
W 17	-		

12 cm = 30 km

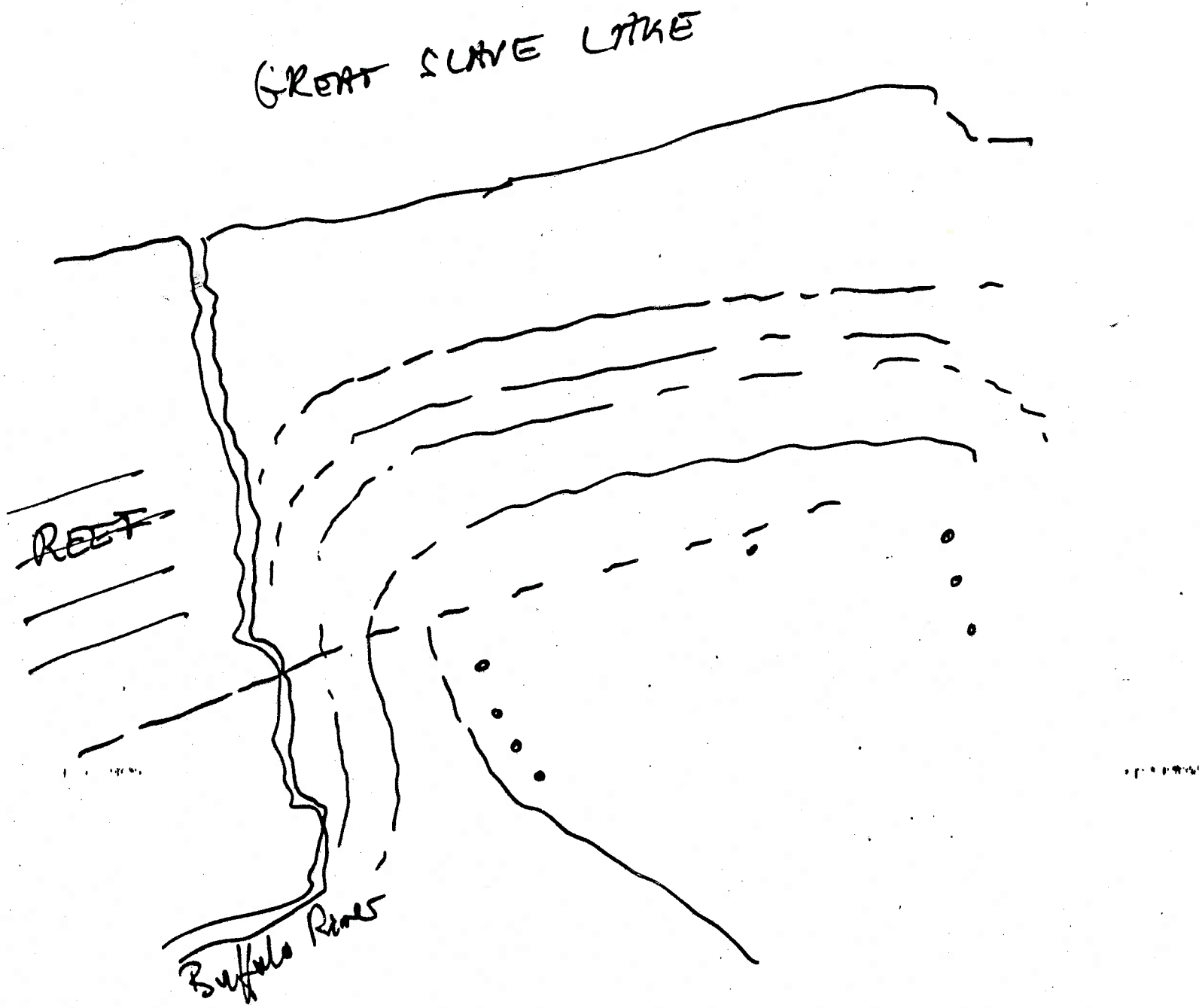
GREAT SLAVE LAKE
REEF
Buffalo River

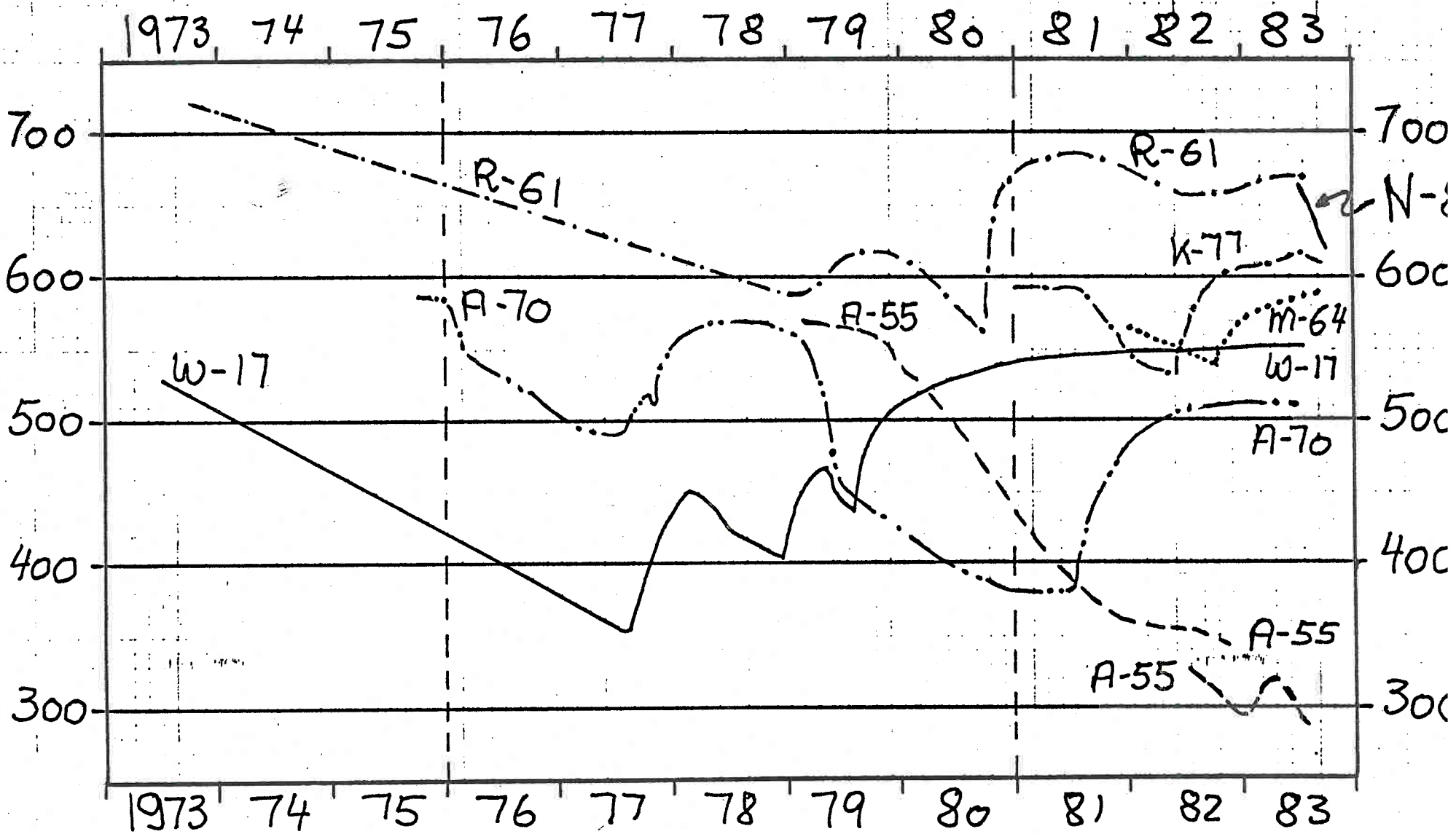
1973
74
75
76
77
78
79
80
81
82
83
700
600
500
400
300
R-61
A-70
A-55
W-17
R-61
K-77
M-64
W-17
A-70
A-55
A-55
N-

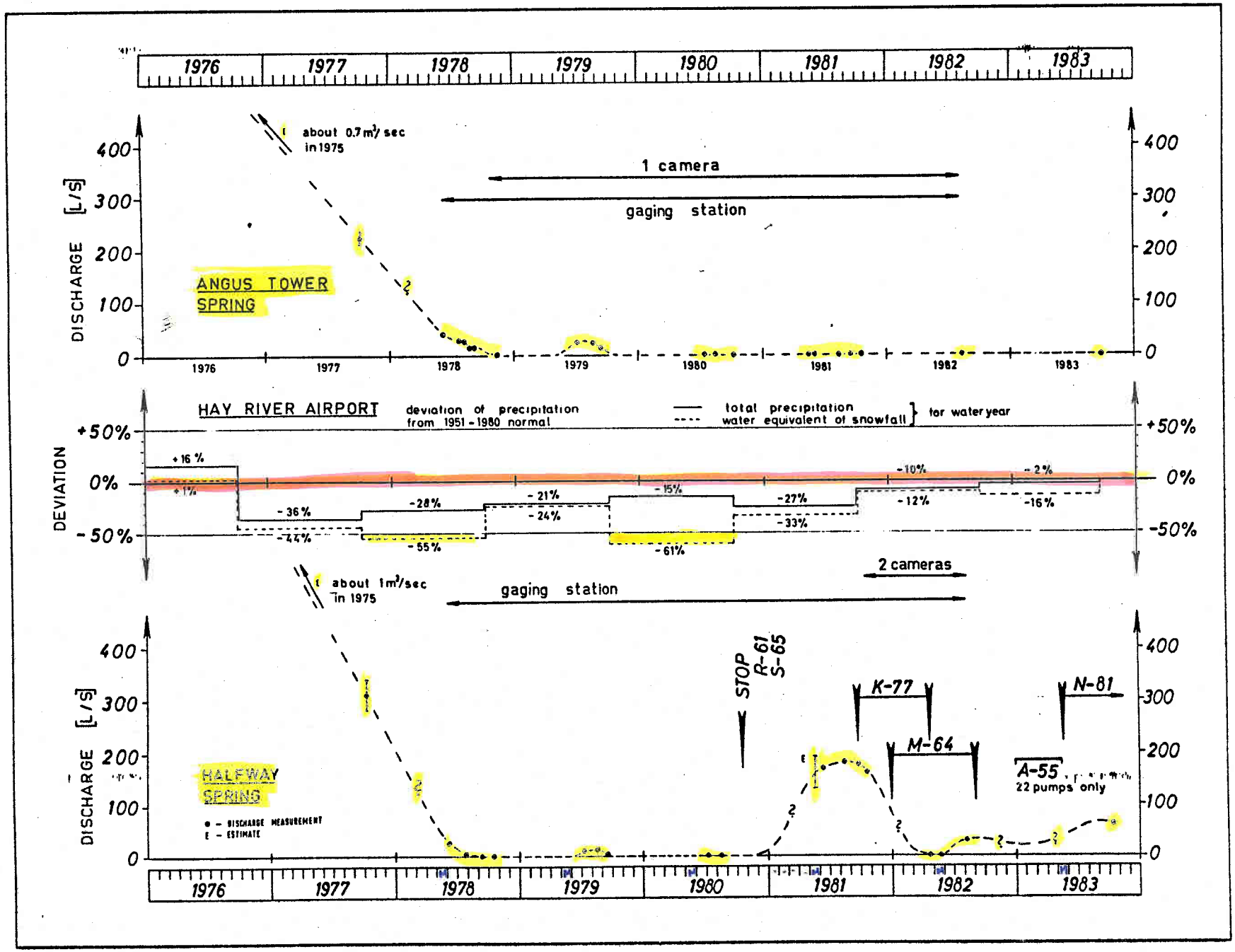
1976
1977
1978
1979
1980
1981
1982
1983
about 0.7 m³/ sec in 1975
1 camera
gaging station
DISCHARGE [L/S]
ANGUS TOWER SPRING
400
300
200
100
0
HAY RIVER AIRPORT
deviation of precipitation from 1951 - 1980 normal
total precipitation
water equivalent of snowfall
for water year
DEVIATION
+50%
0%
-50%
+16 %
+1%
-36 %
-44%
-28%
-55 %
-21%
-24%
-15%
-61%
-27%
-33%
-10%
-12%
-2 %
-16%
about 1m³/sec in 1975
2 cameras
gaging station
STOP
R-61
S-65
K-77
M-64
N-81
A-55
22 pumps only
HALFWAY SPRING
● - DISCHARGE MEASUREMENT
E - ESTIMATE

1971	1968 & 1969[1]	Jan. 20	Feb. 28	Mar. 30	Apr. 30	Jun 1	Jan. 29	Jul. 27	Aug. 31	Sept. 28	Oct. 26	Nov. 30	Dec. 31
Main trend													
K-57	655	585.32	581.57	593.01	587.48	594.52	592.07	588.32	586.29	585.90	585.37	581.79	582.48
J-44	624	542.40	541.57	541.77	540.06	545.82	540.70	541.30	539.51	540.70	538.45	535.98	537.84
N-42	641	557.50	555.84	567.79	567.55	568.39	568.07	567.29	567.67	567.11	567.29	566.23	565.61
O-42	645	561.28	557.84	554.90	567.23	563.31	563.46	562.86	568.75	563.34	562.70	561.54	561.91
M-40	623	579.12				574.40	574.15	573.61	574.37	568.01	564.21	570.70	569.91
P-29	621								594.93	594.95	594.93	594.91	594.80
South trend													
W-17	620										578.33	575.19	574.71
X-15	612	550.23	551.79	550.81	550.44	548.68	546.68	544.16	545.32	545.51	545.35	542.85	540.17

1) water levels [ft] estimated from Pine Point Mines' map "Original water table contours (1968 & 69) and all testholes"

1972	1968 + 1969[1]	Jan. 31	Feb. 29	Mar. 31	Apr. 30	May 31	Jun 30	Jul 31	Aug. 31	Sept. 30	Oct. 31	Nov. 30	Dec. 31
Main trend													
K-57	655	581.94	579.99	579.27	579.92	577.64	589.01	592.88	595.34	594.88	592.10	587.26	588.97
J-44	624	529.85	526.20	528.84	528.54	550.15	567.90	569.32	572.09	573.46	573.99	574.50	
N-42	641	564.60	563.22	561.83	562.08	563.03	571.74	572.14	573.93	576.43	577.19	578.58	578.33
O-42	645	559.83	559.03	556.93	565.38	566.42	574.61	580.54		583.50			
M-40	623	569.08	568.73	566.03	565.89	567.70	573.46	570.46			575.17		
P-29	621	591.74	591.70	591.62	591.53	591.82	592.64	592.57	592.81				
South trend													
W-17	620	574.44	583.20	580.46	579.92		583.24	576.54	573.04	558.13	547.42	546.10	~533
X-15	612	539.79	540.60	542.05	541.88	539.95	542.79	543.39	541.23	536.45	533.68	530.50	526.83

1) water levels [ft] estimated from Pine Point Mines' map "Original water table contours(1968 and 69) and all testholes".

1973	1968+ 1969[1)]	Jan. 30	Feb. 26	Mar.27	Apr.30	May 28	Jul.3	Jul.30	Sept.3	Oct.2	Oct.30	Dec. 3	Dec.31
Main trend													
K-62	652								603.75	603.14		602.51	
K-57	655	581.15	574.44	571.27	571.84	565.97	562.04	557.18	558.84	555.67	557.28	552.95	550.74
N-42	641	579.33	578.49	579.16	579.11	578.88	579.87	580.11					
M-40	623		578.49	579.00	577.35	578.42	579.45	578.96	579.13	579.77	579.92	579.66	
Mill site	600		581.45	581.36	581.04	580.82	582.17	581.02	580.55	581.16	580.74	580.10	582.16
South trend													
R-61	710									722.94	720.14		
W-17	620	534.70	531.64	533.95	533.12	525.56	526.72	522.19	509.29	508.34	506.61	506.79	505.27
X-15	612	524.67	522.50	524.85	526.46	524.98	524.57	523.87	519.68	518.73	516.83	516.95	516.77

1) water levels [ft] estimated from Pine Point Mines' map: "Original water table contours (1968 + 69) and all testholes."

1974	1968 + 1969 [1]	Jan. 28	Mar. 4	May 31	Apr. 28	Jun. 2	Jun. 30	Jul. 28	Aug. 27.	Oct. 1	Nov. 5	Dec. 3	Dec. 31
Main trend													
K-62	652		591.61			592.13	590.91	590.11	589.61	587.48	587.11	587.10	585.73
K-57	655	554.18	545.56	546.66	544.95	540.08	537.35	537.42	527.95	528.08	527.86	526.37	527.44
M-40	623					579.59	578.43	578.51	578.10	577.62	579.58	580.16	579.79
Millsite	600	580.61	580.35	581.38	580.83	581.10	580.11	579.32	580.52	577.88	580.85	579.32	583.94
South trend													
R-61	710							719.11	717.62	715.86	705.98	703.93	704.00
W-17	620	500.12	496.05	490.44	488.61	485.45	478.22	465.86	461.48	460.33	455.80	452.97	455.08
X-15	612	521.19	520.35	522.20	521.34	522.06	518.09	515.27	512.22	510.02	508.83	505.87	504.13

1) Water levels [ft] estimated from Pine Point Mines' map: "Original water table contours (1968 and 69) and all test holes".

1975	1968 + 1969[1)]	Feb. 4	Mar. 4	Apr. 8	Apr. 30	May 26	June 25	July 29	Aug. 26	Sept. 29	Oct. 28	Dec. 2	Dec. 30
South Trend													
S-65	710									692.22	691.37	686.28	682.85
R-61	710	716.16	716.00	701.77	706.83	709.80	701.46	700.96	700.10	693.33	692.05	678.28	674.70
W-17	620	443.80	441.65	442.09	448.12	438.00	432.77	442.43	436.05	430.79	435.59	432.15	426.23
X-15	612	502.42	501.24	500.25	506.10	504.92	499.04	496.14	493.47	491.47	490.38	489.60	487.19
Main Trend													
J-69	660									630.96	629.82	622.32	620.02
H.Z. 3	660									600.92	599.62	590.10	587.36
H.Z. 2	670									622.73	597.18	611.01	608.49
H.Z. 1	660									547.07	542.84	537.08	535.23
K-62	652	584.21	584.69	582.24	582.31	581.89	575.15	567.79	566.87	551.53	555.67	542.55	540.13
K-57	655	521.49	520.45	519.15	529.23	518.51	516.28	508.00	523.63	540.44	549.74	553.23	552.99
M-40	623	579.00	579.74	578.40	578.67	578.39	578.28	579.41	579.08	579.05	578.93	578.21	577.34
Mill site	600	579.04	579.26	579.00									
North Trend													
A-70	610										586.59	585.81	584.74
A-55	615									586.16	586.50	586.29	585.81

1) Water levels [ft] estimated from Pine Point Mines' map" "Original water table contours (1968 + 69) and all testholes".

1976	1968+ 1969[1])	Jan. 28	Mar 2	Mar. 30	Apr. 27	Jun. 1	June 29	Jul. 28	Aug. 31	Sept. 28	Nov. 2	Nov. 30	Dec. 28
South trend													
S-65	710	682.57	679.00	675.54	674.75	678.05	682.44	677.15	674.52	674.15	672.46	670.21	669.91
R-61	710	673.52	673.20	672.84	672.92	669.13	677.71	666.45	665.87	665.13	656.34	653.87	650.48
T-58	720		712.58	712.04	715.21	716.27	723.48	713.76	704.62	704.90	701.69	699.51	698.50
W-17 #16	620	422.71	422.84	420.52	424.94	420.04	421.17	415.63	411.41	410.59	404.56	401.66	391.07
X-15W #13	612	485.55	484.04	483.31	483.26	484.58	480.94	486.12	482.45	482.16	479.62	478.44	475.35
X-15E	612												
Main trend													
N-81	695												
K-77	677												
J-69	660	619.28	615.35	614.80	612.56	611.01	610.84	610.64	608.58	606.78	605.73	604.98	606.08
H.Z.4	665												
H.Z.3	660	586.56		576.95									
M-64	670												
H.Z.2	660	607.56	603.89	603.18	600.91	598.44		596.47	595.98	596.08	593.36	592.00	604.08
H.Z.1	660	534.70	532.50	530.72	525.11	523.77	523.63	519.78	515.25				
K-62	652	539.11	536.13	535.60	530.13	518.56	529.18	520.08	520.29	518.40	501.00	552.30	564.87
K-57	655	557.30	552.18	554.87	558.39	557.64	556.76					551.50	556.02
M-40	623	577.20	576.67	575.67	575.00		578.35	574.59	573.40	573.64	573.09	571.42	571.56
Millsite 9	600										558.02	559.58	557.79
BH 6076	685												
Bush camp	650												
North trend													
W8SN	580												
A-70	610	583.19	548.59	545.71	549.92	538.00	533.84	534.80	531.87	531.08	512.69	510.55	508.43
Z-64N	600												
A-55 #13	615	584.88	581.31	581.79	580.57	578.95	578.28	575.25	575.50	574.36	574.31	572.56	572.23
A-55 TH	615												

1) water levels [ft] estimated from Pine Point Mines' map: "Original water table contours (1968 + 69) and all testholes".

1977	1968 + 1969 [1]	Feb. 1	Mar. 1	Mar. 28	Apr. 26	May 31	Jun. 28	Aug. 2	Aug. 30	Sept. 27	Nov. 1	Nov. 29	Dec.
South trend													
S-65	710	668.62	668.56	667.15	664.61	660.29	659.76	656.02	653.12	650.46	648.75	646.77	
R-61	710	651.80	661.12	656.71		634.69	634.07					615.50	615.71
T-58	720	696.38	696.38	694.38	682.22	672.49	673.25	671.90	667.56	655.11	655.25	639.85	636.08
W-17 #16	620	389.99	388.12	389.12	386.94	383.01	372.15	358.00			400.14	405.15	402.51
X-15W #13)	612												
X-15E)	612	480.12	478.80	478.11	476.62	460.48	458.44	456.03	453.78	455.39	451.61	446.39	
						474.21	471.64	471.34	468.63	468.03	466.93		463.64
Main trend													
N-81	695												
K-77	677												
J-69	660	608.54	609.35	609.07	607.32	606.98	606.63	605.57	604.82	606.58	606.52	584.47	571.40
H.Z.4	665												
H.Z.3	660												
M-64	670												
H.Z.2	660	604.44		607.66	606.96	607.03	606.54	606.26	606.30	606.11	606.79	603.56	595.52
H.Z.1	660												
K-62	652	570.64	574.34	576.07			579.30	580.01	578.61	582.13	582.57		
K-57	655	561.17	4.17	567.31	568.14		571.54	572.87					577.91
M-40	623	570.30	569.86	568.76	567.64	567.66	567.35	566.41	565.08	565.29	564.25	563.42	563.06
Millsite 9	600	556.70	557.47	556.96	553.21	555.06	555.19	554.50	553.56	553.45	551.14	550.62	550.08
BH 6076	685												
Bush camp	650												
North trend													
W-85N	580												
A-70	610	499.45	491.92	493.58	489.00	493.48	490.53	489.01	519.91	521.48		539.31	556.08
Z-64N	600												
A-55 #13	615	571.59	570.85	570.32	568.66	569.02	567.12	567.78		569.39			
A-55 TH	615												

1) water levels [ft] estimated from Pine Point Mines' map: "Original water table contours (1968 + 69) and all testholes".

1978	1968 + 1969[1)]	Jan.	Feb.	March	April	May	June	July	Aug.	Sept.	Oct.	Nov.	Dec.
South trend													
S-65	710												
R-61	710	617.82	620.92	613.11	610.26	606.20	602.91	604.08	601.66	597.96	598.01	595.37	593.82
T-58	720	633.34	635.08	630.99	627.21	626.64	627.20	612.72	613.49	607.82	607.86	604.16	607.45
W-17 #16	620	403.14	449.46	445.29	441.07	437.69	417.63	415.15	410.81	405.19	404.62	403.18	399.14
X-15W #13)	612		451.85	459.25	458.69	459.23	445.46	437.50	437.82	434.81	432.54	431.30	429.49
X-15E)	612	463.44	467.00	471.18	470.66	472.09	470.06	466.05	463.95				
Main trend													
N-81	695												
K-77	677												
J-69	660	562.16	559.38	556.83	553.42	550.51	552.95	551.30	546.00	536.91	522.42	517.31	513.25
H.Z.4	665											556.35	553.19
H.Z.3	660											556.21	550.15
M-64	670												
H.Z.2	660	590.53	586.97	584.55	582.01	578.49	577.55	576.03	574.79	574.01	571.32	571.52	564.14
H.Z.1	660												
K-62	652												
K-57	655	578.71	579.55	580.81	581.14	581.83	582.22	582.48	582.58	583.08	583.63	583.54	583.04
M-40	623	562.73	562.69	563.15	562.81	562.42	562.25	563.30	561.92	562.06	562.02	561.47	561.47
Millsite 9	600	550.41	550.79	550.40	549.96	549.55	549.91	551.24	549.14	549.23			
BH 6076	685												
Bush camp	630												
North trend													
W-85N	580												
A-70	610	563.05	569.49	572.11	572.98	574.12	574.76	575.57	574.92	575.32	575.43	574.88	573.10
Z-64N	600												
A-55 #13)	615							573.50	573.57	573.76	574.45	574.31	574.19
A-55 TH)	615												

1) water levels [ft] estimated from Pine Point Mines' map: "Original water table contours (1968 + 69) and all testholes".

1979	1968 + 1969[1)]	Jan.	Feb.	March	Apr. 30	May 28	July 2	Aug. 1	Sept. 14	Oct. 8	Oct. 29	Nov. 26	Dec. 31
South trend													
S-65	710	642.53	643.69	644.89						650.38	650.26	649.49	652.15
R-61	710	590.95	602.12	609.11	620.67	614.07	613.18	622.24	607.33	600.45	604.70	602.35	617.94
T-58	720	605.97	652.06	664.07	666.35	670.43	673.35	673.91	670.01	669.00	669.10	668.75	673.31
W-17 #16	620	432.26	456.40	468.75	472.69	442.94	436.02	433.15	483.74	475.73	498.64	504.65	512.46
X-15W #13	612	430.84	446.67	449.44	466.12	464.97	462.97	461.05	477.62	482.09	483.56	494.08	501.28
X-15E	612												
Main trend													
N-81	695												
K-77	677												
J-69	660	513.50	516.40	515.92	514.37	514.13	512.14	511.71	503.16	500.62	546.29	559.68	569.40
H.Z.4	665	551.90	552.38	552.00	552.40	561.44	549.62	548.74		543.69	553.08	564.64	572.86
H.Z.3	660	543.64	548.51	548.37	548.09	547.41	544.73	544.91	541.10	540.80	548.58	559.81	570.83
M-64	670												
H.Z.2	660	562.36	561.70	561.65	561.13	560.98	559.67	558.39	556.09	555.00	554.73	560.03	569.97
H.Z.1	660					566.27	562.85	559.82		557.14	555.90	553.99	555.42
K-62	652												
K-27	655	582.91	582.70	582.09	581.60	581.04	579.10	577.32	574.17	573.20	570.16	567.69	567.23
M-40	623	561.19	561.02	560.43	559.38	559.66	559.62	558.46	557.79	557.76	556.81		
Millsite 9	600							557.11	556.03	556.66	555.61	554.58	555.94
BH 6076	685												
Bush camp	650												
North Trend													
W-85N													
A-70	610	572.57	572.57	559.14	512.84	498.00	479.17	476.92	464.27	463.77	446.75	434.68	434.77
Z-64N	600												
A-55 #13	615	574.12	573.91	574.21	572.87	569.31		563.98		560.60	558.38	557.05	541.65
A-55TH	615												

1) water levels [ft] estimated from Pine Point Mines' map: "Original water table contours (1968 + 69) and all testholes".

1980	1968 + 1969[1]	Jan. 28	Feb. 25	Mar. 31	Apr. 25	May 29	June 26	Jul. 31	Aug. 25	Sept. 25	Oct. 31	Nov. 29	Dec. 19
South trend													
S-65	710	649.12	645.00		659.39	634.00	629.66				659.89	671.85	675.08
R-61	710	616.43	617.55	606.98	605.69	595.28	594.45	589.12			646.44	665.20	670.42
T-58	720	672.12	673.84	671.60	669.52	666.89	663.86	661.61	661.43	657.07	667.91	683.47	687.91
W-17 #16	620	516.43	518.04	521.76	526.96	527.96	530.59	531.26	533.86	537.30	537.30	539.69	540.45
X-15W #13	612	502.98	506.24	509.23	512.03	514.17	515.17	510.91	513.73	517.50	517.59	520.49	521.02
X-15E	612												
Main trend													
N-81	695												
K-77	677					598.20	598.02	596.90	596.54	596.42	591.38	595.10	595.00
J-69	660	572.05	574.56	577.19	577.62	578.32	578.17	576.88	576.82	575.28	575.13	577.84	578.68
H.Z.4	665	572.62	578.80	583.25	581.34	581.95	578.52	580.00	579.96	578.60			
H.Z.3	660	572.05	575.06	577.83	578.90	580.11	581.05	580.02	578.88	578.84	579.42	582.17	583.19
M-64	670												
H.Z.2	660	569.92	572.98	575.68	577.11	576.82	576.07						
H.Z.1	660	552.70	554.31	553.90	555.27	554.80	551.35	553.66	551.94	551.43	549.68	549.85	549.06
K-62	652									549.90	547.92	547.88	547.06
K-57	655	564.60	563.99	563.10	563.50	561.06	560.34	558.64	559.23	557.68	555.02	554.71	553.19
M-40	623												
Millsite 9	600	554.01	555.47	554.14	553.48	553.73	552.24	552.54	550.71	551.13	550.46	552.59	549.22
BH 6076	685												
Bush camp	650												
North trend													
W-85N	580												
A-70	610	430.84	422.44	427.99	405.54	396.40						381.43	385.63
Z-64N	600												
A-55 #13)	615	539.20	537.16	530.88	519.65	504.19	492.17	485.44	466.48	457.90	452.66	446.81	438.41
A-55 TH)	615												

1) water levels [ft] estimated from Pine Point Mines' map: "Original water table contours (1968 + 69) and all testholes".

1981	1968 + 1969[1)]	Jan. 28	Mar. 10	Apr. 1	May 4	June 1	June 30	Aug. 4	Aug. 31	Oct. 5	Nov. 4	Nov. 30
South trend												
S-65	710	679.82	680.35	682.95	683.66	684.25	684.54	689.89	685.04	684.10		
R-61	710	678.03	681.56	682.48	683.58	683.98	679.53	684.21	684.55	683.91		
T-58	720	694.24	697.37	698.42	699.70	702.84	701.66	701.74	702.48	702.14		
W-17 #16	620	544.36	543.61	544.24	545.22	545.19	545.85	546.21	544.20	543.85		
X-15W #13	612	523.20	524.69	525.36	527.79	526.99	527.78	528.61	530.11	529.64		
X-15E	612											
Main trend												
N-81	695											
K-77	677	596.04	598.83	596.32	595.94	594.65	594.93	594.50	582.84	576.96	545.98	549.70
J-69	660	580.96	581.97	582.37	582.10	581.18	581.02	581.02	580.70	580.13		
H.Z.4	665				590.70	589.92	589.92	589.24	589.68	585.45		
H.Z.3	660	586.07	587.54	588.87	589.06	587.40	587.00	586.40	586.03	585.37		
M-64	670							585.26	585.05	584.35	584.77	572.19
H.Z.2	660				585.49	584.89	584.81	584.11	584.07	583.32		
H.Z.1	660	547.03	547.38	546.52	546.68	544.95	(553.98)		542.09	540.93		
K-62	652	546.00	547.03	545.03	544.50	542.39	541.22	540.55	538.57	537.24		
K-57	655	550.30	547.29	547.15	545.85	542.99	541.27	539.74	536.63	533.93		
M-40	623											
Millsite 9	600	548.00	546.35	545.97	545.33	542.62	542.12	540.86	540.41	538.22	536.09	535.73
BH 6076	685											
Bush camp	630											
North trend												
W-85N	580											
A-70	610	381.41	379.23	376.36	376.70	381.88	380.60	378.08	397.10	428.72	451.89	472.51
Z-64 N	600								443.62	448.55	456.13	458.74
A-55 #13	615	431.63	427.69	423.95	421.70	409.23	408.81	386.57	381.94	370.81	364.20	360.71
A-55 TH	615											

1) water levels [ft] estimated from Pine Point Mines' map: "Original water table contours (1968 + 69) and all testholes".

1982	1968 + 1969[1)]	Jan. 12	Feb. 15	Mar. 1	Apr. 6/7	May 3/4	May 26/27	July 5	Aug. 10	Aug. 30	Sept. 27	Oct. 29	Nov. 29
South trend													
S-65	710		674.64		669.12	666.49	665.18	667.03	664.05	664.00	663.48	663.86	665.53
R-61	710		675.30	672.28	668.76	665.76	666.44	660.43	659.47	659.01	658.57	658.11	659.85
T-58	720			696.57	693.79	692.14	691.55	690.07	689.33	689.05	688.78	688.37	688.77
W-17 #16	620	549.20	549.55	550.20	550.40	550.74	551.00	551.39	550.00	551.95	552.28	552.99	553.39
X-15W #13	612	532.19	533.83	534.74	535.35	535.54	536.40	536.99	535.67	533.32	538.18	538.93	539.63
X-15E	612												
Main trend													
N-81	695						(603.49)	636.10	637.66	642.97	646.87	646.01	628.88
K-77	677	545.04	538.24	537.24	537.45	536.55	529.84	577.48	589.45	593.36	596.64	594.70	600.33
J-69	660	568.49	566.44	564.98	561.68	559.86	555.26	556.63	558.61		559.91	559.91	567.81
H.Z.4	665	585.75	586.10	567.13	564.34	562.54	559.31	557.21	556.66	556.85	556.16		
H.Z.3	660	564.72	562.15	560.10									
M-64	670	562.02	559.42	557.72	554.31	555.94	551.72	548.32	547.04	546.21	542.96	548.67	565.24
H.Z.2	660	564.28	564.56	561.96	559.11	554.74		547.94	546.37	545.47			
H.Z.1	660	535.88	535.33	534.23	532.71	532.15	531.66	530.68	529.76	529.14	528.35	527.78	528.97
K-62	652	534.90	532.36	532.48	531.20	531.12	530.97	529.92	530.02	528.43	527.67	520.38	528.44
K-57	655	534.78	528.06	528.66	528.81	(535.27)	523.15	521.83	521.13	520.48	519.60	518.68	518.22
M-40	623												
Millsite 9	600	534.63	533.08	533.50	530.38	527.87	531.58	530.64	529.91	529.38	528.55	524.07	528.20
BH 6076	685												
Bush camp	650						606.69	605.34	610.18	612.11	614.74	618.19	619.14
North trend													
W-85N	580		547.70										
A-70	610	492.46	496.31	496.69	500.10	501.07	542.06	555.01	560.95	563.27	565.04	565.04	567.93
Z-64N	600	470.52	473.53	468.87		472.95	502.40	502.08	502.99	503.93	503.91	504.42	504.17
A-55 #13	615	361.56	360.57	357.67	354.11	352.95	474.36	474.17	476.75	480.93	476.85	474.40	470.87
A-55 TH	615						355.75	354.95					
								325.21	322.29	312.62	307.78	296.95	297.21

1) water levels [ft] estimated from Pine Point Mines' map: "Original water table contours (1968 + 69) and all testholes".

1983	1968 + 1969[1)]	Jan. 4	Feb. 1	Mar. 3	Apr 2	May 2	Jul 7	Aug. 12/15	Sept. 19/20	Oct. 3/4	Nov. 7/8	Dec. 5/7
South trend												
S-65	710	667.32				673.0	675.94		675.42	675.62	675.30	
R-61	710	661.67				667.7	670.69		672.56	673.14	673.19	
T-58	720	689.44				692.2	694.70		695.06	695.31	695.32	
W-17 #16	620	554.61				554.3		555.33	555.31	555.81	555.67	555.95
X-15W #13	612	540.98				541.7		542.97	543.30	543.55	543.58	543.87
X-15E	612											
Main trend												
N-81	695	655.43				661.2		595.75	574.28	565.77	579.83	578.93
K-77	677	604.51				611.7	613.9	605.05	600.94	598.94	596.98	596.66
J-69	660	574.42				586.8	591.67	597.70	593.04	594.18	594.42	594.85
H.Z.4	665											
H.Z.3	660											
M-64	670	572.11				585.1	590.0	592.25	593.65	594.70	595.14	596.37
H.Z.2	660											
H.Z.1	660	530.94							541.66	542.51	542.35	
K-62	652	530.93				537.8		541.80	542.63	543.33	543.51	
K-57	655	517.14				517.7		525.52	525.47	526.18	525.61	525.92
M-40	623								525.23	525.38	524.06	524.10
Millsite 9	600	524.28				527.2	527.44	524.61	520.33	522.23	519.52	519.87
BH 6076	685					635.9	588.58					
Bush camp	650	620.06					626.40	624.59		620.66	618.04	
North trend												
W-85N	580	569.14					578.34	576.41	575.02	574.92	573.66	
A-70	610	504.49				507.5	509.32	510.30	509.75	510.00	509.08	508.82
Z-64N	600	475.08				488.5	485.93	486.02	477.77	477.16	475.85	476.55
A-55#13)	615											
A-55TH)	615	294.88	310.38	310.7	316.85	302.9	305.76	289.13	285.78	285.78	274.72	271.45

1) water levels [ft] estimated from Pine Point Mines' map: "Original water table contours (1968 + 69) and all testholes".

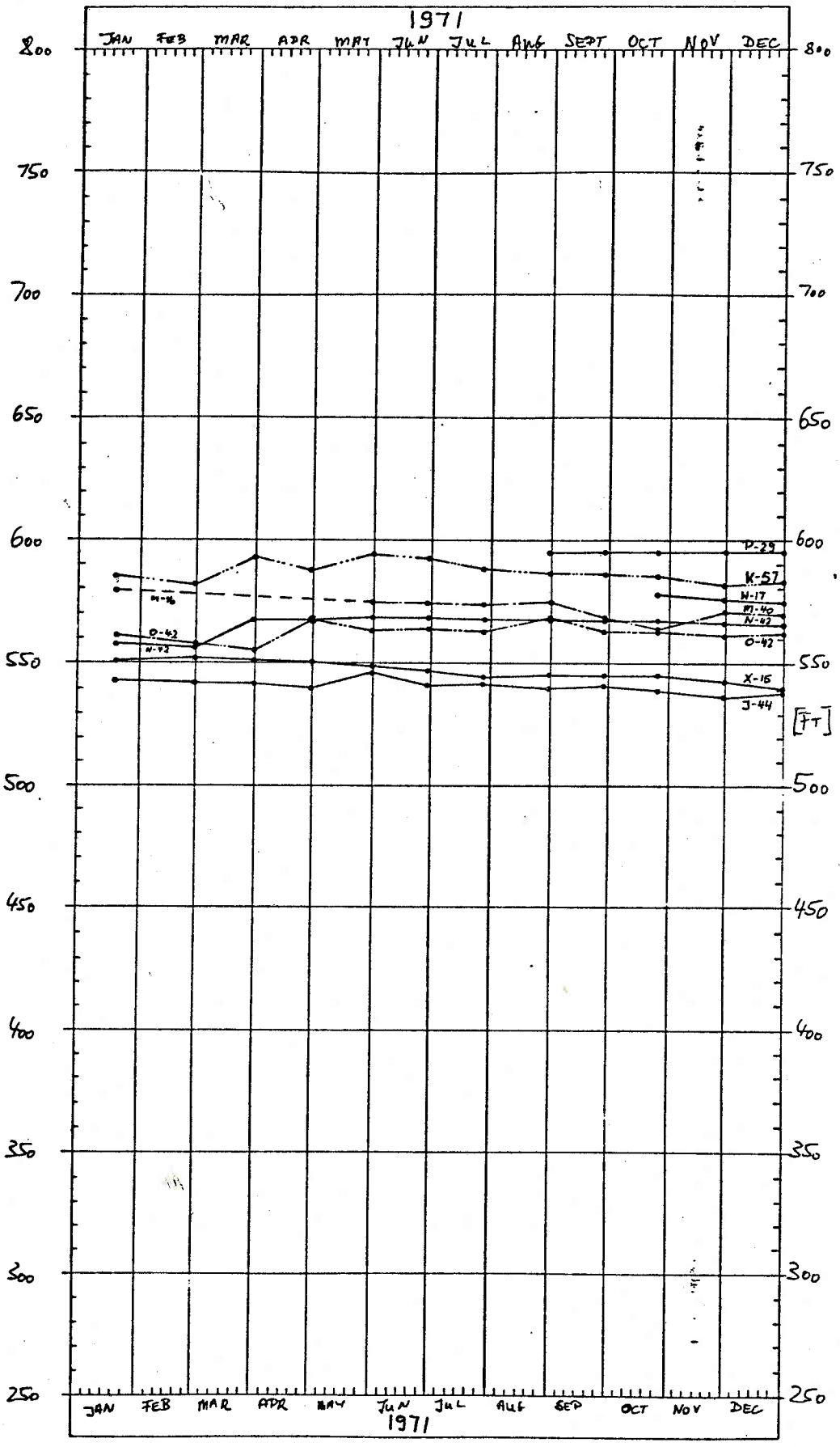
1971
JAN
FEB
MAR
APR
MAY
JUN
JUL
AUG
SEPT
OCT
NOV
DEC
800
750
700
650
600
550
500
450
400
350
300
250
D-29
K-57
N-17
M-40
N-42
O-42
X-15
J-44
O-42
N-42
[FT]
1971

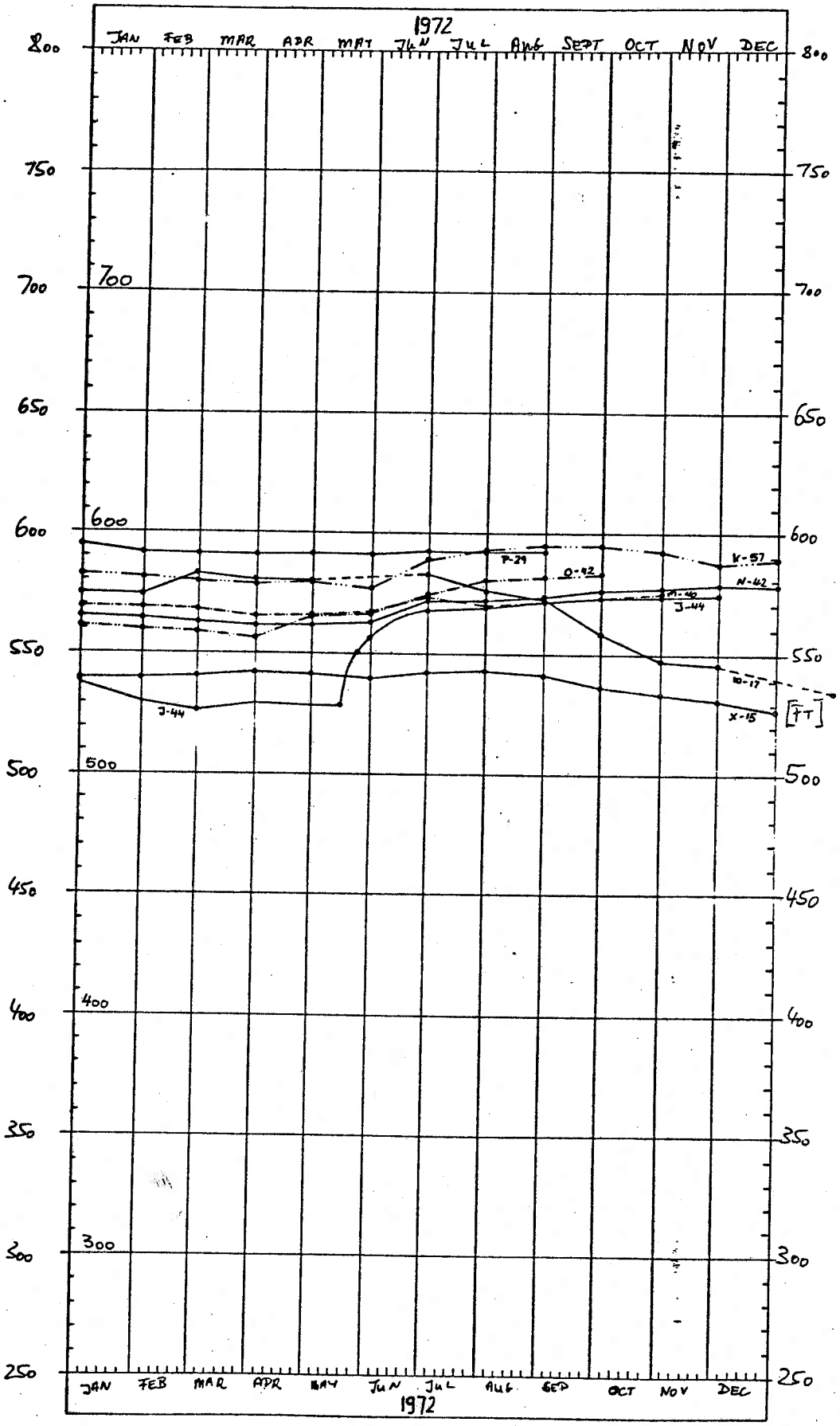
1972
JAN FEB MAR APR MAY JUN JUL AUG SEPT OCT NOV DEC
800
750
700
650
600
550
500
450
400
350
300
250
P-29
O-42
V-57
N-42
M-40
J-44
J-44
R-17
X-15
JAN FEB MAR APR MAY JUN JUL AUG SEP OCT NOV DEC
1972